UNIVERSITY OF OKLAHOMA

GRADUATE COLLEGE

ADDITIVE MANUFACTURING OF LOW-TEMPERATURE CO-FIRED CERAMICS FOR MICROWAVE APPLICATIONS

A THESIS

SUBMITTED TO THE GRADUATE FACULTY

in partial fulfillment of the requirements for the

Degree of

MASTER OF SCIENCE

By

MARVIN BENGE

Norman, Oklahoma

2016

ADDITIVE MANUFACTURING OF LOW-TEMPERATURE CO-FIRED CERAMICS FOR MICROWAVE APPLICATIONS

A THESIS APPROVED FOR THE
SCHOOL OF ELECTRICAL AND COMPUTER ENGINEERING

BY

Dr. Hjalti Sigmarsson, Chair

Dr. Jessica Ruyle

Dr. Caleb Fulton

I would like to dedicate this thesis to my father. I would not be the person I am today without him in my life. Also to my grandparents for treating me like a son and continuous encouragement.

Acknowledgements

I would first like to thank my advisor, Dr. Hjalti Sigmarsson for his continued support and encouragement. From initially taking his electrical circuits class during my junior year to the writing of this thesis, he has always had an open door.

I would also like to thank Dr. Jessica Ruyle and Dr. Caleb Fulton for their support. I have learned a great deal from the members of my committee and will be forever grateful for the guidance, both academic and life, that I have received during my academic career. To each of you, thank you.

This research was supported by a grant from the Research Council of the University of Oklahoma Norman Campus.

The materials used in this research were provided by Heraeus Precious Metals North America Conshohocken LLC.

Lastly, I would like to thank Phil Fisher at Omega Micro Technologies for discussions relating to LTCC processing.

Table of Contents

List of Tables

List of Figures

Abstract

Additive manufacturing (AM) technologies enable fabrication of structures directly from CAD files. Due to these technologies adding material one layer at a time, complex, 3D structures can be realized. The microwave industry has utilized various AM techniques to fabricate devices including antennas, filters, and transmission lines. Unfortunately, these techniques are limited to printing a single type of material. This limitation often requires for additional processing of the devices such as metallization before they become functional.

Low temperature co-fired ceramics (LTCC) is a technology commonly used to create a variety of high-frequency devices. The main benefits LTCC devices are reliability, low loss, hermetic, multi-layer, and ability to withstand extreme temperatures. Current LTCC fabrication requires numerous specialized machines and is expensive for low-volume productions due to the labor intensive manufacturing process. Due to the fabrication process of LTCC, prototyping with this technology is not easily achieve.

This thesis will present an alternative to current AM techniques allowing for the realization of multi-layer, multi-material LTCC devices. The fabrication process is presented along with the devices produced. The presented process has the ability to yield rapidly prototyped LTCC devices, which has not been previously achievable.

1 Motivation, Background, and Previous Work

In today's rapidly advancing scientific community, there are several areas where current technologies are still limiting further advancements. One of these limitations is the ability to directly transform a computer-aided design (CAD) into a physical, measurable device. Although this gap has been dramatically reduced by advancements in the additive manufacturing industry, there is a gap to be bridged in rapidly manufacturing high-frequency devices, more specific, multi-layer, multi-material devices.

Low temperature co-fired ceramics (LTCC) refers to a process capable of producing multi-layer, multi-material electrical and even mechanical devices that are often used in high frequency applications. By using ceramic layers and high conductivity metals, compact and low-loss electrical devices can be realized. Although LTCC devices have excellent electrical properties, the technology has some drawbacks. Due to the manufacturing process being both labor-intensive and process-intensive, they can be quite costly to manufacture and can have a several week turnaround time.

In the future, instead of having to wait weeks for an LTCC prototype to be fabricated, it could possible to fabricate such a device in-house in only a few days. This reduction in fabrication time would allow multiple iterations of a device. Not only would the fabrication time be drastically reduced, but also the cost. This is achieved by altering the fabrication process used to create a prototype. Instead of using traditional LTCC techniques, additive manufacturing techniques will be implemented.

This process would be an invaluable resource to researchers designing devices based on LTCC. The ability to completely fabricate an LTCC device in-house at a fraction of the time and cost. This process would allow for devices to be realized

that were not previously due to high costs. This process would also allow lower budget projects to take advantage of the features of LTCC.

The objective of this study is to merge two well-established techniques into a process that can be used to create low-cost, rapidly manufactured devices for a fraction of current cost. The base materials used are the exact materials that are used in LTCC manufacturing. While the material remains the same, the preparation and processing is different. Instead of casting the material into sheets that must be handled and process individually, the material remains a viscous slurry and it is printed using conventional additive manufacturing techniques.

The process to rapidly prototype an LTCC device would be an excellent tool for researchers. It would allow a design to be transformed from a digital drawing directly into a physical, measurable device in a matter of days instead of weeks. Unlike current practices, a device could be revised numerous times without having to wait weeks between builds. This increase in speed and convenience as well as a decrease in cost has the potential to yield better designs.

In order to realize such a process, not only the materials must determined but also the additive manufacturing techniques. The goal is to create a process that can be used to create an LTCC devices using a 3D printer. The printer would dispense the conductive layers as in [1], and also the dielectric layers. This additive manufacturing approach to the fabrication of LTCC devices is much less complex and involved than the traditional techniques, which are described in the following section. A brief overview of the additive manufacturing is also provided in the chapter. By employing additive manufacturing techniques to fabricate LTCC devices, researchers will have the ability to fabricate such devices in-house quicker and cheaper compared to previous techniques.

1.1 Traditional LTCC Manufacturing

In the microelectronics industry there are two processes mainly used for creating circuits: thin film and thick film. In thin film processing, very thin layers 200Å to 20,000Å are deposited onto a substrate by vacuum evaporation, sputtering, chemical vapor deposition, or similar high-precision methods. While thin film processing offers excellent precision, it does so at high costs and typically requires a high-end clean room. Thick film is more common to be used in devices that don't require nanometer accuracy. Thick film processing begins with a pre-fired substrate, such as alumina. Layers are printing using screen printing techniques and firing nominally occurs between layers. Although thick film has been widely used in the electronics industry, it does have limitations. As a result of each layer of the device being fired prior to the printing of the next layer, adhesion of the layers is weakened. Thick film processes evolved into high temperature co-fired ceramics (HTCC) and low temperature co-fired ceramics.

HTCC addresses the fabrication shortcomings of traditional thick film practices while introducing a few of its own limitations. Instead of starting the fabrication with a pre-fired substrate, the substrate is un-fired or green. This allows of better adhesion between layers. By the ceramic layer being green, it must also be sintered during the firing, and as a result the firing temperature is increased from 850^{o}C to 1600^{o}C. As a result of this temperature increase, refractory metals such as tungsten, manganese, and molybdenum must be used. Although these metals have a high melting point, they also have higher resistivity. Furthermore, due to oxidation of the refractory metals, the atmosphere in the oven during firing must be composed of hydrogen. Although HTCC provides added benefits to thick film processing, it also has disadvantages due largely to the required sintering temperature of alumina.

LTCC combines the benefits of HTCC as well as the benefits of thick film pro-

cessing. Although LTCC is co-fired like HTCC, it is sintered at 850^{o}C. This allows for non-refractory metals such as silver, gold, and copper to be used. The sintering is also done without the presents of an inert gas thus reducing the complexity and cost. LTCC is easier and cheaper to manufacture than HTCC as well as having lower losses.

Since the early 1980s when LTCC technology was developed by Hughes and Dupont [2], the technology has been expanded and applied to many different types of devices. Although this technology was originally developed for military systems, it has found uses in many fields of engineering. Due to its hermetic design and ability to withstand extreme temperatures, devices made with this technology can be found on automobiles, airplanes, rockets, space vehicles, and consumer electronics, to name a few.

Although LTCC is well suited for many applications, its often not the first choice of manufactures. This is due to the complex and tedious manufacturing process which will be explained below. For simplicity, the process is divided into nine steps. Figure 1.1 shows the equipment necessary in LTCC fabrication.

1. Slurry Preperation

   In order to produce the LTCC tapes, the required materials are mixed together into a slurry. The slurry is created by combining ceramic particles, glass phase, binder, plasticiser, solvent, and dispersant. Each component added has a functional purposed required either in the fabrication of LTCC or for a desired property. For example, glass phase or frit has a very simple yet critical function. Without glass phase in the tapes, the sintering temperature would be around 1600^{o}C, the sintering temperature of HTCC. By adding glass, the sintering temperature is reduced to less than 900^{o}C, and in doing so allows for cheaper less exotic metals, such as silver, instead of refractory metals.

Figure 1.1: Traditional LTCC manufacturing equipment; images taken from Keko Equipment [3]

Once the slurry has been mixed, it is added to a container and ready for tape casting.

2. Tape Casting

   Tape casting refers to the process which transforms the slurry into a thin sheet known as tape. This process requires a specialized piece of equipment. The mechanics of the machine at a basic level are simple. A large vat containing the slurry is loaded into the machine. The slurry is then dispensed onto a carrier film such as mylar and a "doctor blade" controls the thickness of the tape. The wet tape is then dried and rolled in such a fashion that it can be transported and used at a later date. Although this is a simple machine it is very large in size, up to 20m in length.

3. Blanking & Drying

   Tape manufactures recommend preconditioning of LTCC tapes before they are used. The purpose of this is to drive out any remaining solvents and also release stresses attributed to tape casting. This is done either by heating the tapes using a hot air oven or by placing in a nitrogen dry box for 24 hours. Once a device has been precondition a blanking die is used to create orientation marks along with alignment holes. [4]

4. Via Formation

   Vias are conductive paths between two tape layers and are generally created by mechanical punching or laser drilling. In industry and precision builds, mechanical punching is preferred due to its high quality and consistency where laser drilling is best suited in rapid prototyping. Once all the vias have been created they must be filled with the appropriate material.

5. Via Fill Printing

In this step the void that was created by punching the hole in the previous step is filled with material, most commonly silver or other similar conductor. The via is filled using common thick-film techniques including screen printing or stenciling.

6. Pattern Printing

   Similar to the previous stage where vias were filled, thick-film techniques are used in printing the patterns onto the layers of tape. Using alignment holes in the tape, the screen must a precisely position. These patterns can include transmission lines, inductors, capacitors, filters or virtually any desired two-dimensional pattern. Once the pattern has been printed, the layer in inspected visually for any defects.

7. Stacking

   Each of the previous steps has been preparing each layer of the device individually. During this step the layers are combined and aligned to prepare for lamination. This is often done using alignment holes and is the final step where each layer can be individually inspected.

8. Laminating

   The purpose of this step is to unite each of the green tape layers into a single unified multi-layer piece. This is done by using one of a few different methods. One of which is uniaxial lamination. This method involves using a hydraulic press with heated plates. A typical laminating profile applies approximately 3000 psi with the plates at 70^{o}C for 10 minutes. The other commonly used method is isostatic lamination. The temperature and pressure are the same as uniaxial, but the pressure is applied uniformly by water pressure.

9. Co-Firing

   The term co-firing refers to the practice of firing the device only once and sintering the device as a whole. This has many advantages including creating a hermetic multi-layer device. During this stage, all the organic material is burned out of the layers.

1.2 Additive Manufacturing

Additive manufacturing refers to the process in which material is added layer-by-layer to create a 3D object. These technologies have several advantages including increased fabrication freedom as well as reduction in build time compared to subtractive manufacturing techniques such as milling.

Additive manufacturing dates back to the early 1980s when Charles Hull, the inventor of 3D printing and founder of 3D Systems, began investigating the forming of 3D objects from a fluid medium. The process was described in the patent originally submitted in 1984 as,

> Briefly, and in general terms, the present invention provides a new and improved system for generating a three-dimensional object by forming successive, adjacent, cross-sectional laminae of that object at the surface of a fluid medium capable of altering its physical state in response to appropriate synergistic stimulation, the successive laminae being automatically integrated as they are formed to define the desired three-dimensional object. [5]

While the technology has rapidly developed in the last 30 years, the basic principles have not changed. Modern-day 3D printers still create devices one layer at a time.

The American Society of the International Association for Testing and Materials (ASTM) published [6] standardizing terminologies used in additive manufacturing. In doing so, the technical committee (F42) divided the additive manufacturing into seven categories in which today's 3D printers are classified including: binder jetting, directed energy deposition, material extrusion, material jetting, powder bed fusion, sheet lamination, and vat photopolymerization. A brief description of these categories as well as related technologies is presented in Table 1.1. An illustration of each category can be seen in Figure 1.2.

Table 1.1: Additive Manufacturing Process Categories by ASTM F42 [6]

Process Type	**Brief Description**	**Related Technologies**	**Materials**
Binder Jetting	A liquid bonding agent is selectively deposited to join powder materials	Powder bed and injet head, plaster-based 3D printing	Polymers, foundry sand, metals
Directed Energy Deposition	Focused thermal energy is used to fuse materials by melting as they are being deposited	Laser metal deposition	Metals
Material Extrusion	Material is selectively dispensed through a nozzle or orifice	Fused deposition modeling (FDM)	Polymers
Material Jetting	Droplets of build material are selectively deposited	Multi-jet modeling	Polymers, waxes
Powder Bed Fusion	Thermal energy selectively fuses regions of a powder bed	Electron beam melting, selective laser sintering (SLS), selective heat sintering	Metals, polymers
Sheet Lamination	Sheets of material are bonded to form an object	Laminated object manufacturing, ultrasonic consolidation	Paper, Metals
Vat Photopolymerization	Liquid photopolymer in a vat is selectively cured by light-activated polymerization	Stereolithography (SLA), digital light processing	Photopolymers

In recent years, 3D printers have become more readily available. For example, a researcher can purchase a fused-deposition modeling (FDM) based 3D printer for under $1000; however, these devices have low-resolution layers ($\geq 100\mu$m) and not well suited for high-frequency applications. Another shortcoming of FDM is directly related to the plastic-type material that is melted and extruded into layers. While this provides a low-cost option for some uses, it cannot be used in applications where temperatures exceed the melting point of the material which is 105^{o}C

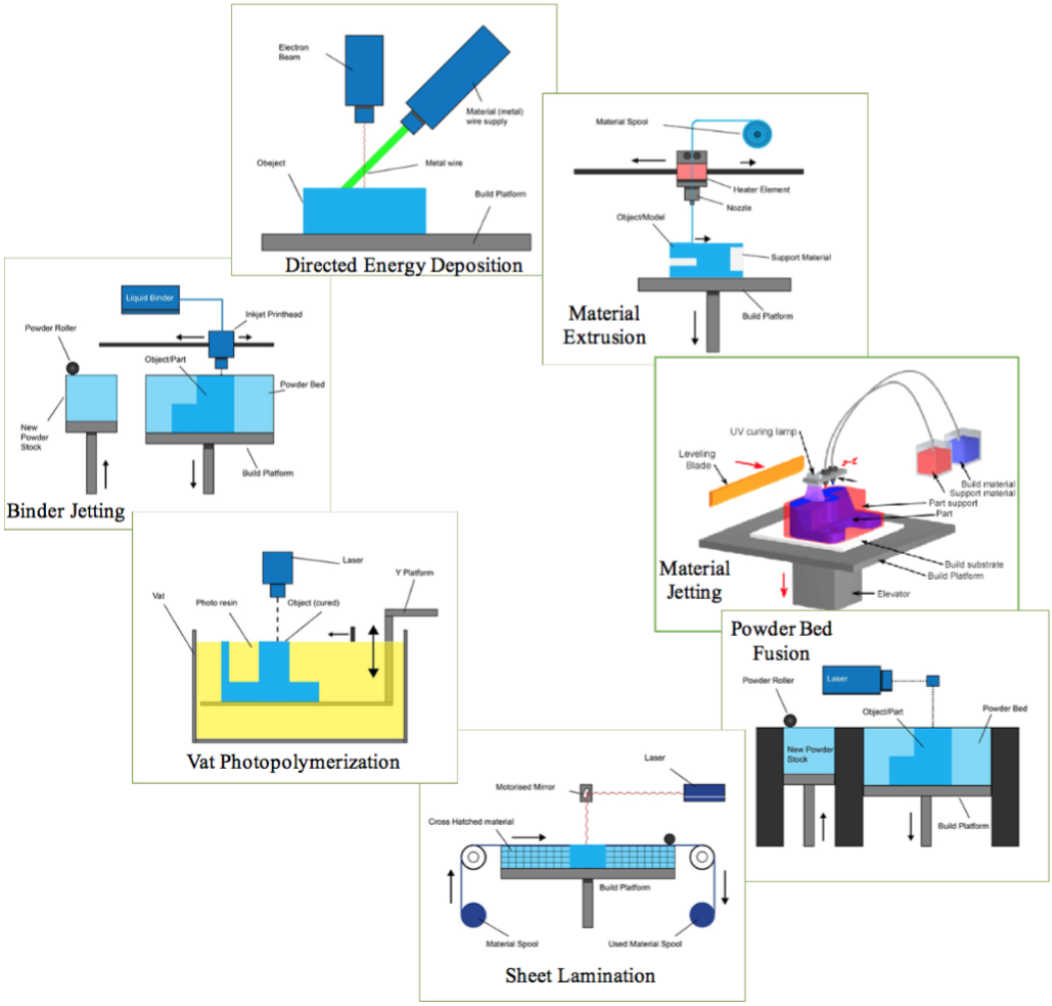

Figure 1.2: Illustrations of additive manufacturing categories compiled from [7]

for ABS, the most-commonly used material. FDM does have an advantage over other AM techniques. Due to the method used to dispense the material, it is easier to allow multiple materials to be dispensed. Stratasys, a company specializing in office-based rapid prototyping, has utilized this feature to create soluble support structures. Instead of having to remove supports tediously by hand, they can be printed from an from a second head, and dissolved away after the build has completed.

Another additive manufacturing technique better suited for high-frequency ap-

plications is stereolithography apparatus or SLA. Instead of using heat to melt the material and form layers, SLA uses photo-reactive resin as well as a light source and scanner to create layers. SLA has a much greater resolution, and it can print many different types of materials, including ceramic. This type of additive manufacturing has been used to create various high frequency devices [8]–[12]. The University of Michigan has used this method to create complex ceramic antennas, including a ceramic waveguide fed luneburg lens reported of having a 24-dB of gain in [13] and an 8x8 dielectric resonator antenna array [14].

This AM technique has also been employed by Purdue University to create 3D high frequency components including a low-loss embedded cavity in [15] as well as Ku band horn antennas that were later metalized with conductive ink. The average return loss from the horns is above 20 dB throughout the band of operation [8]. The University of South Florida has also explored the use of stereolithography to fabricate microwave devices including an electrically small 3D cube antenna [11]. It can be seen that this method can be used to create very complex and intricate structures, but has one main disadvantage; the use of only one material, meaning the use of conductive materials in buried layers is difficult to achieve.

Similar to SLA in that only one material can be used, selective laser sintering or SLS has also been used to create high-frequency devices. Instead of being limited to dielectric layers as in SLA, SLS can only be used to create metal 3D objects. This limits its microwave applications to conductor only devices such as waveguides. This technology has been used to create the WR90 X-Band waveguide, shown in Figure 1.4 having comparable loss to a commercially available waveguide [17].

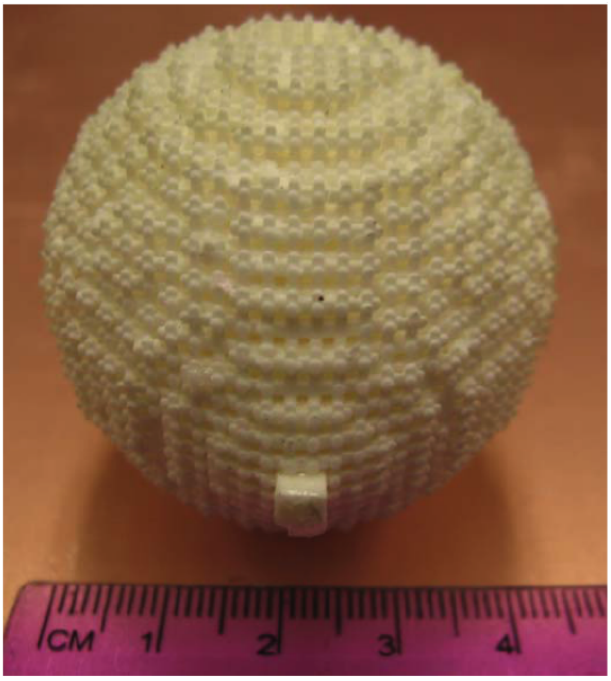

Figure 1.3: Luneberg Lens Ceramic Antenna Produced Using SLA in [16]

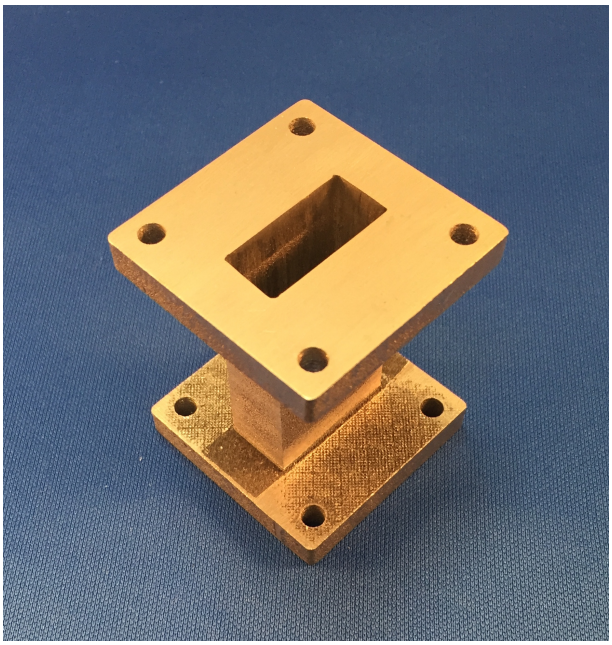

Figure 1.4: SLS WR90 waveguide

1.3 Overview of Present Work

Although LTCC is traditionally not manufacturing using additive manufacturing techniques it has been an area of research in recent years. In 2013 nScrypt, a leading manufacturing of micro-dispensing printers, investigated the use of LTCC materials to create a 2D thermal management structure. The fabrication details along with results were presented in [18].

The equipment used in [18] included a nScrypt 3Dn-Tabletop 3D printer. The ceramic powder used was produced from Dupont 951 green tape. The tape was heated to 450^{o}C for 4 hours to burn out all of the organic matter found in the tape. The purpose of this was to breakdown the tape so it could be made into a powder. This powder was then combined with a polymer binder to create a ceramic paste that could be dispensed. The ”951 paste” along with carbon paste was used to create samples of the designed thermal management structure. Unfortunately the samples were unable to be successfully sintered. After several experiments varying the sintering profile the cracking was reduced and the samples wouldn't break apart but cracking still occurred.

The University of South Florida has also applied micro-dispensing techniques to microwave components. In [19] an RF front end consisting of a circularly polarized dipole antenna, filter, and phase shifter was realized. The dielectric and conductive layers were printed with an nScrypt.

Honeywell Federal Manufacturing and Technologies along with Sandia National Laboratories has also investigated additive manufacturing LTCC. Contrary to the investigations conducted by nScrypt, only the conductive layers were dispensed in [1]. While approach does have the ability to yield high quality layers and has the potential for reducing production time and waste, it still relies on LTCC tapes. In doing so, the variable of dielectric layer fluctuation is nearly eliminated.

2 Fabrication

In order to have the ability to additively manufacture LTCC devices, the fabrication technique as well as the equipment has to be determined. These determinations will be made based on a series of experiments and their findings. This section is divided into two categories: a broad overview of the fabrication process and the supporting experiments used for evaluating the process.

The method of additive manufacturing used can be best described as micro-dispensing; material is dispensed using pressure and a small orifice to place the material on the desired surface. This method is found to be the most viable option due to the ability to use multiple materials in a controlled way. The process steps include slurry preparation, slurry printing, conductor printing, and co-firing. Details of each step will be found in the following subsections.

2.1 Slurry Preparation

The initial step in the fabrication process is preparing the ceramic slurry. The slurry was composed of three elements, Heraeus X-200W ceramic, Sartomer SR238 monomer, and Variquat CC55 dispersant. The sole purpose of creating the ceramic slurry is to transform the ceramic powder into a product that could be dispensed to create layers.

After numerous experiments varying the mixing concentrations of ceramic in the slurry, the conclusion is that a dispersant is necessary. Without a dispersant the slurry is unable to be uniformly mixed and is clumpy, dry and not viscous. The absents of the dispersant can also be noticed in a fired sample. Figure 2.1 is a comparison of two fired samples, the one on the left is without a dispersant, and the one on the right contains a dispersant. The dispersant also allows the slurry to become free-flowing and uniformly mixed allowing the slurry to be dispensed.

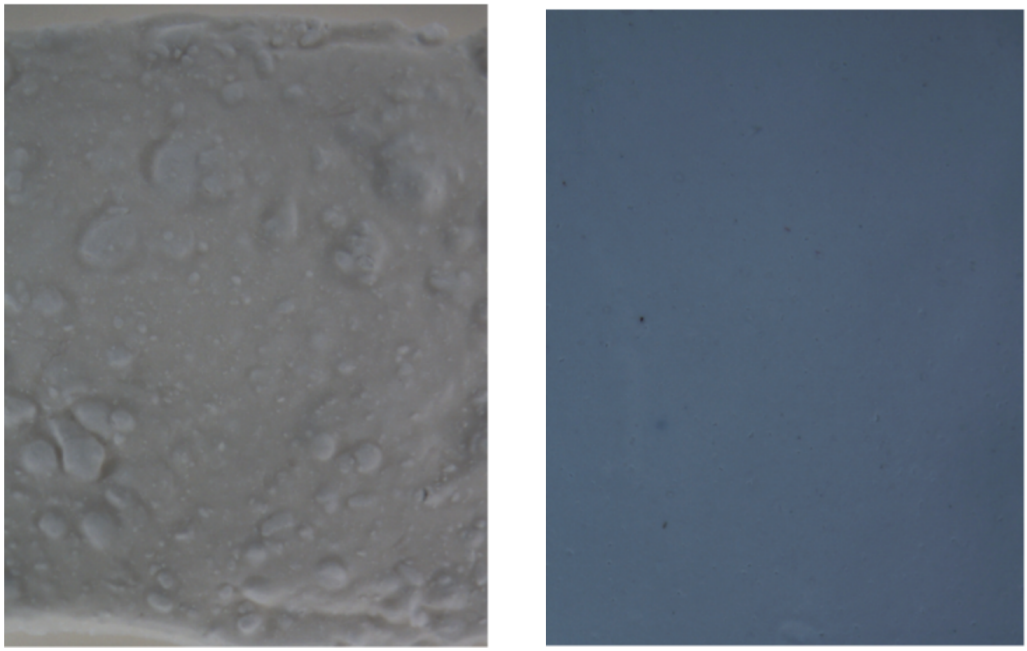

(a) Without Dispersant (b) With Dispersant

Figure 2.1: Dispersant comparison in fired samples

It was observed that after the ceramic slurry was left undisturbed for several hours, it would begin to separate leaving the ceramic particles on the bottom and the top clear. The slurry could be easily remixed in less than a minute. This settling is due to the ceramic being heavier and falling to the bottom of the mixture.

The slurry is created by adding the appropriate amount of ceramic powder, monomer, and dispersant into a jar and mixing until uniformly distributed. Mixing is achieved using a ball mill along with a stainless spoon to agitate the mixture periodically. Although slower incremental mixing was investigated, it was found that it did not provide any benefits over adding the material all at once.

The recipe used calls for the ceramic loading to be 50% by volume. Initial experiments were conducted using this ratio, but was later modified to allow for an improved sintered layers. The ceramic slurry that was found the yield the best results was loaded with 60% of its composition being ceramic. The sintered sam-

ples have minimal bowing and are not cracked. The only problem with the 10% increase in ceramic is the increase in viscosity requiring the printer to be adjusted. Based on the creation of a slurry that can be printed and fired without noticeable imperfections, it can be concluded that this is a viable material to produce ceramic layers.

2.2 Printing Slurry

Once the slurry has been prepared, the next step is printing the slurry into layers using a printer. For this step the fabricated 3D printer will be used; Section 3.1 contains details about the printer. There were many obstacles that had to be overcome in order for a layer to be successfully printed including adhesion of the slurry, thickness limitations, uneven layers, and even the process to print a layer had to be developed.

The slurry is printed using a syringe, needle, and pneumatic dispenser with variable pressure control as well as vacuum. This method allowed for acceptable flow control of the slurry as well as variable diameter of the dispensing needle. The syringe was attached to the printer using a syringe holder designed to be used on an LPKF milling machine. The ceramic was printed onto various different printing platforms including alumina sheets, PTFE sheet and substrate, and even copper. Out of the attempted platforms, a piece of metal with a thin sheet of PTFE material adhered to the top had the least number of drawbacks. The main concern with this method is the care that must be taken to remove the printed sample from the platform prior to firing. This is due to the melting points of the sheet metal and the layer of PTFE compared to the sintering temperature.

Due to the dispensing capabilities of the current printer along with the properties of the ceramic slurry it is difficult to print multiple ceramic layers. When trying to

print layers, caution must be taken to prevent the layer from becoming too thick. This is a common limitation even in traditional LTCC tapes. This becomes even more problematic when printing a ceramic layer on top of a already dried ceramic layer; the wet material does not flow like the initial layer on the PTFE causing the second layer to become too thick to dry without cracking. Furthermore, the first layer is too fragile to allow the wet material on top to be coerced to disperse.

2.3 Conductor Printing

The silver traces were printed using the above-mentioned methods. The main difference between printing silver and the ceramic slurry is the quantity of material being dispensed; silver layers require significantly less material. As a result, the needle must remain at a constant, close distance from the ceramic layer.

The conducting material used in these experiments is a silver paste, part number TC2306) provided by Heraeus. Before the silver could be printed, the viscosity of the paste needed to be reduced by thinning the paste. This allowed the silver to be printed using smaller needles. For example, if a line was designed to be 0.515mm wide, a 27-gauge could be used to dispense a trace having a width of 0.55mm. Figure 2.2 shows the width of an actual printed trace on ceramic using the 27-gauge needle; the printed width was 0.545mm $\pm$ 0.01mm.

To demonstrate a typical setup for printing silver, Figure 2.3 was taken during the conductor print stage of a microstrip ring resonator printed on a 25 mil alumina sheet.

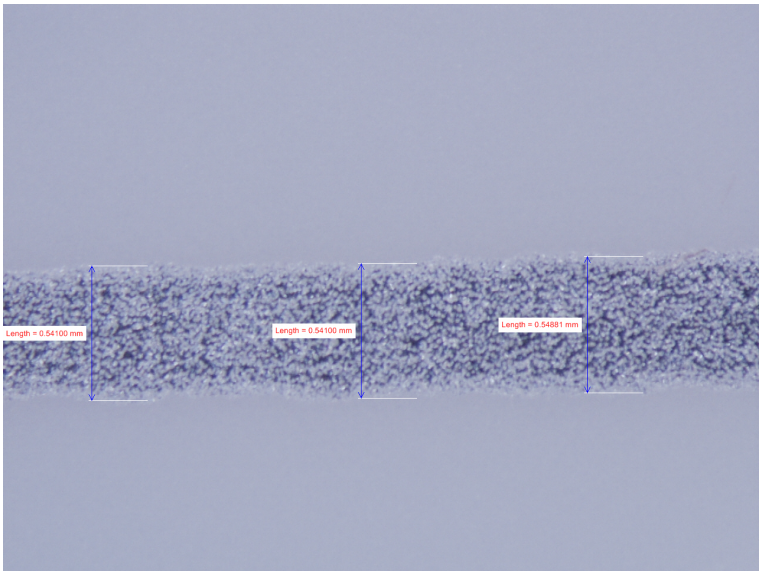

Figure 2.2: Microscope width measurement of post-fired microstrip feed line

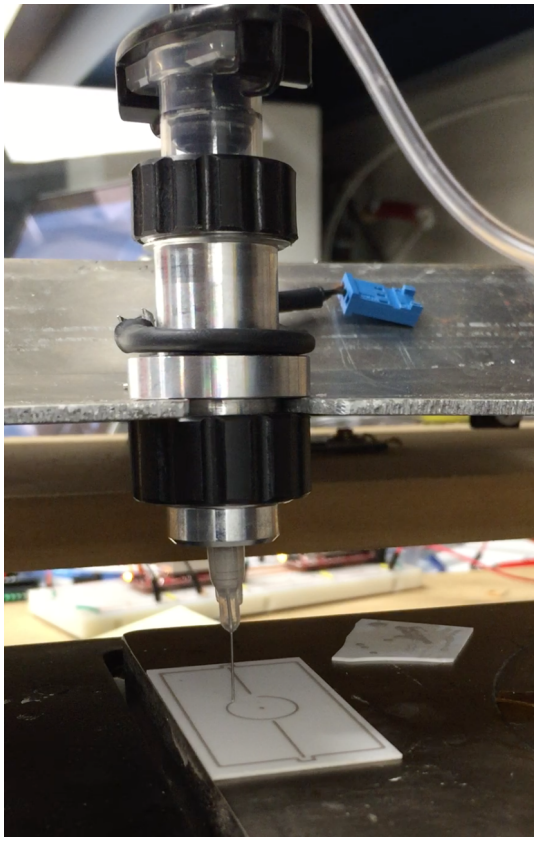

Figure 2.3: Picture taken during the printing of a ring resonator

2.4 Co-Firing

One of the main objectives of the project was to be able to create a device that was able to be co-fired meaning the ceramic and the silver layers would be fired simultaneously. In order to achieve this, an oven with the ability to reach nearly 900^{o}C at a controlled rate, and have programmable dwell durations was required.

Based on the temperature requirements as well as the power readily available in the laboratory, a Vulcan 3-130 box furnace was procured. The specifications of this oven exceeded the requirements by having a maximum temperature of 1100^{o}C, 4.6”W x 5.7”H x 5.2”D fire-able box, as well as only requiring 120VAC. This oven also has the ability to control the temperature, rate of change, and dwell duration which allows the oven to dwell at a lower temperature, near 400^{o}C, to burn out the organic material from printed material. Figure 2.5 shows a plot of the temperature of a complete fire cycle taken using a home-made data logger consisting of a thermocouple and an Arduino.

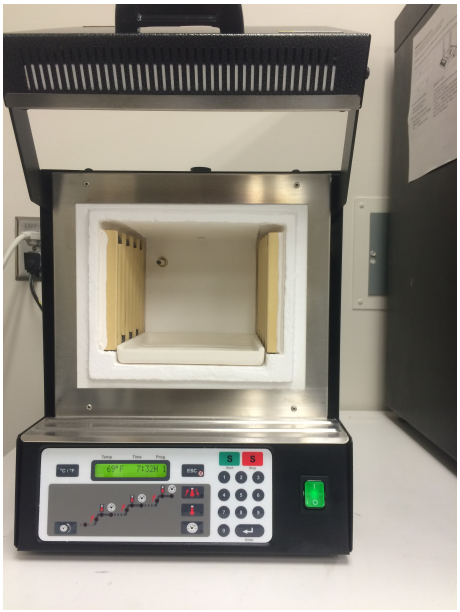

Figure 2.4: Labratory box furnace used to sinter samples

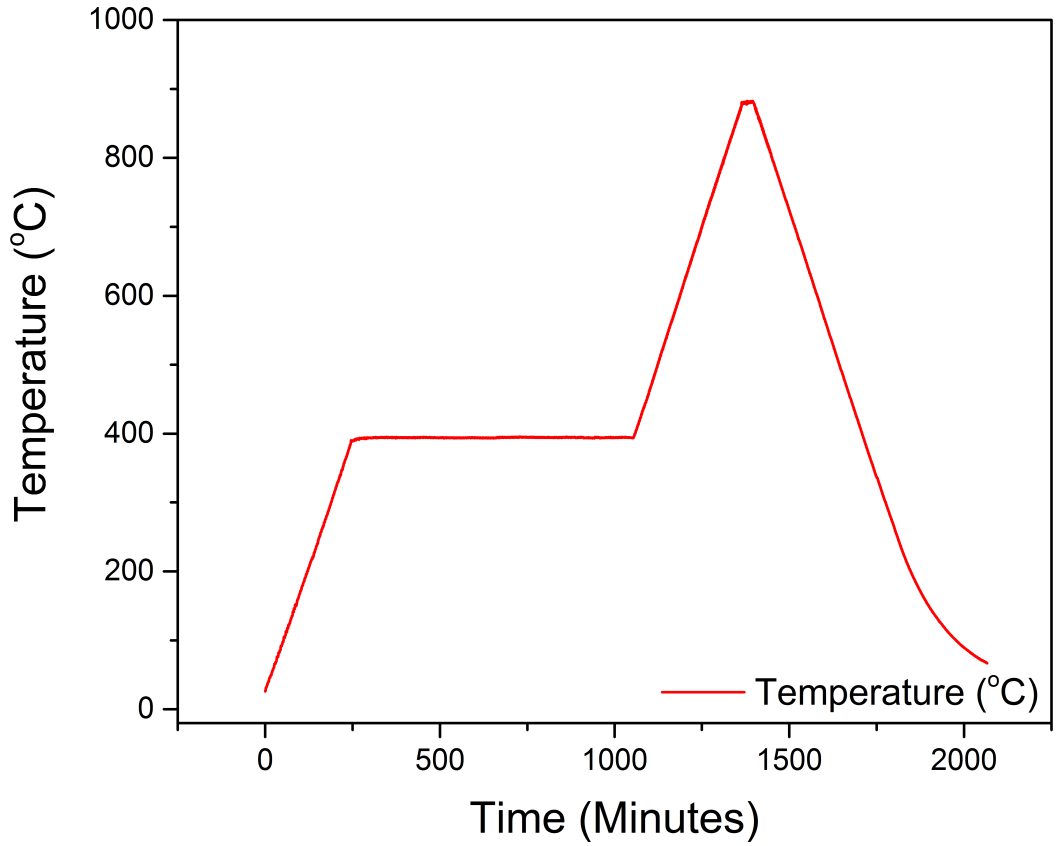

Figure 2.5: Temperature log of typical co-fire cycle

2.5 Process Experiments

Appendix B contains a compilation of the experiments that provided the greatest impact to the project. Included for each experiment is the goal, a brief description, as well as the results. Table 2.1 is an overview of the experiments included in the appendix.

Table 2.1: Overview of experiments

Experiment Category	**Goal of Experiments**	**Results**
Slurry	Create a viscous ceramic slurry that can be printed, dried, and fired without the presents of defects.	A ceramic slurry was developed using ceramic powder, monomer, and dispersant. The slurry was able to be dispensed using the printer and dried without cracking. After increasing the ceramic loading to 60%, it could also be sucessfully sintered.
Ceramic	Establish the processing steps required to fabricate ceramic layers. This includes printing layers, drying layers, as well as sintering layers.	The findings of these experiments allowed for ceramic layers to be sucessfully fabricated. The layers should be vacuumed prior to drying at 125°C to remove air from layer. Once the layer was dry, another layer could be printing to create a multi-layer part. The final step is co-firing at 870°C.
Silver	Determine procedure for printing silver layers. These layers allow for multi-material devices to be realized.	Silver layers can be printing onto dried ceramic layers and sintered without the occurrence of cracking or other defects in the part. Although silver layers are co-fired with the ceramic layers, they must be dried at a cooler temperature, 80°C.
Build Platform	Find a platform the wet slurry could be printing onto, dried, and removed without cracking the dried sample.	Based on the investigations conducted, a PTFE layer adhered to a metal sheet was the best available option. This platform allowed for adequate heat transfer to dry the slurry as well as non-stick properties needed to remove the dried sample.
Printer Fabrication	Design and fabricate a printer that could be used to dispense ceramic and silver layers.	A printer was created using recycled and low cost parts. By removing the belts from an injet printer in conjunction with 1.8° stepper motors, a high resolution (19 steps/mm) 3D printer was fabricated
Design Verification	Verify the proposed designs would functional as antixipated. This includes the ring resonator as well as the proposed fabrication process.	The ring resonator design was verified by using traditional etching techniques to create the device. Furthermore, the LTCC materials were verified by creating a series of samples including DC and RF devices.

Based on the results from the above experiments, it can be said that the process to print a multi-layer, multi-material device has been developed.

3 Design

In the presented research there were two main devices that had to be designed. The first device designed was a printer allow LTCC layers to be additively manufactured. The second device was a microwave resonator. Microwave resonators are often described quality factor (Q). Q indicates energy stored relative to the amount of energy lost within the system.

3.1 Printer

At the inception of this project, the printer to be used was a nScrypt 3D printer. The nScrypt has excellent dimensional resolution as well as pico-liter dispensing accuracy. Unfortunately due to the printer cost, approximately $250,000, it was not procured during the time this study was taking place. Instead, a printer was built using available parts in the lab. Although this device was not as accurate or precise as the nScrypt, it was sufficient to show proof of concept of the idea.

The platform of the printer was originally designed to be a pick and place table used for placing small electronic components. This platform seemed promising due to it having two sets perpendicular rails that would be well suited for x and y-axis. The gantry was able to cover approximately 36mm wide and 28mm deep. The construction of this platform was composed of medium-density fibreboard (MDF) and metal rails. While this was sufficient for the less precise application of placing components by hand it was difficult to zero the z-axis throughout the platform. This was due largely to the wide span of the platform leading to bowing in the middle of the rails.

In order to make this platform functional for printing purposes, a mechanism to move the stage along the axes had to be designed. To achieve this, an inkjet printer was disassembled and inspected for useful parts. The belt, belt tensioner

and stepper motor were removed and mounted to the platform such that it could move the stage of the printer along the x-axis. The same process was conducted for the y-axis of the printer. Figure 3.1 shows the inkjet gantry setup used. The stepper motors were controlled using EasyDriver stepper motor drivers and an Arduino Uno to interface with a computer via a serial connection.

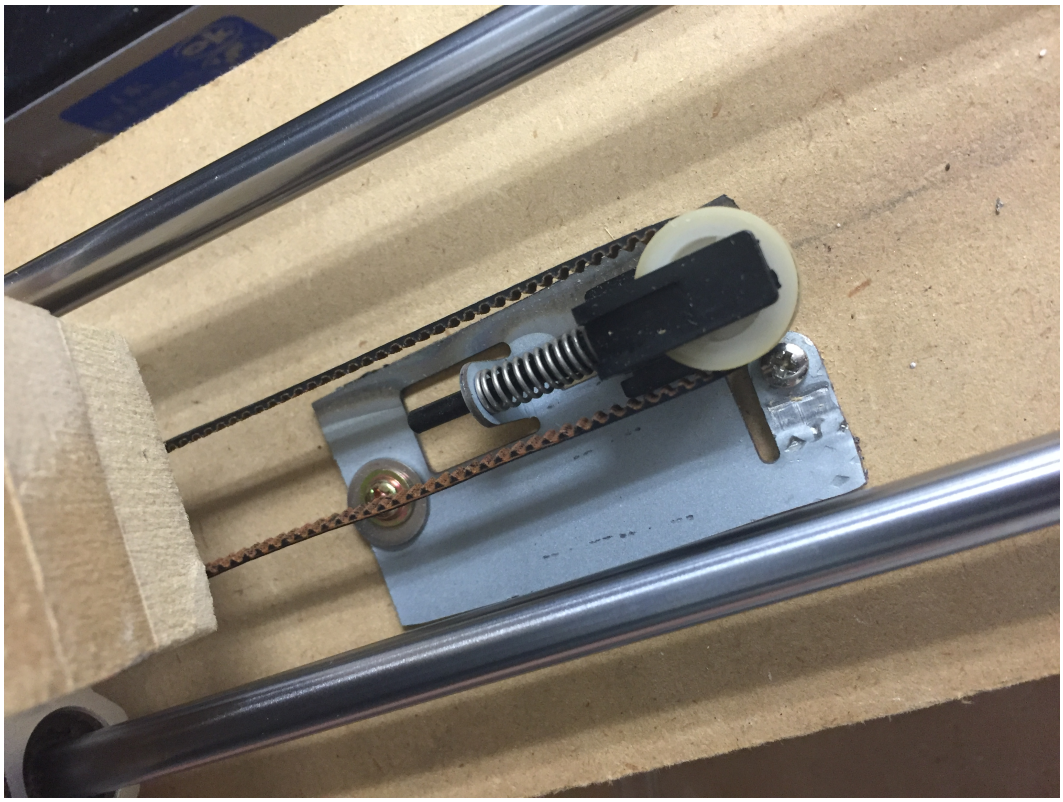

Figure 3.1: Ink-jet belt and pulley used on 3D printer

Unfortunately due to the low quality of the ink-jet stepper motors, they had to replaced. The new stepper motors were larger than the original but had 1.8^o steps. As a result of the motors being larger, the y-axis motor had to be mounted upside down. Figure 3.2 shows final printer setup.

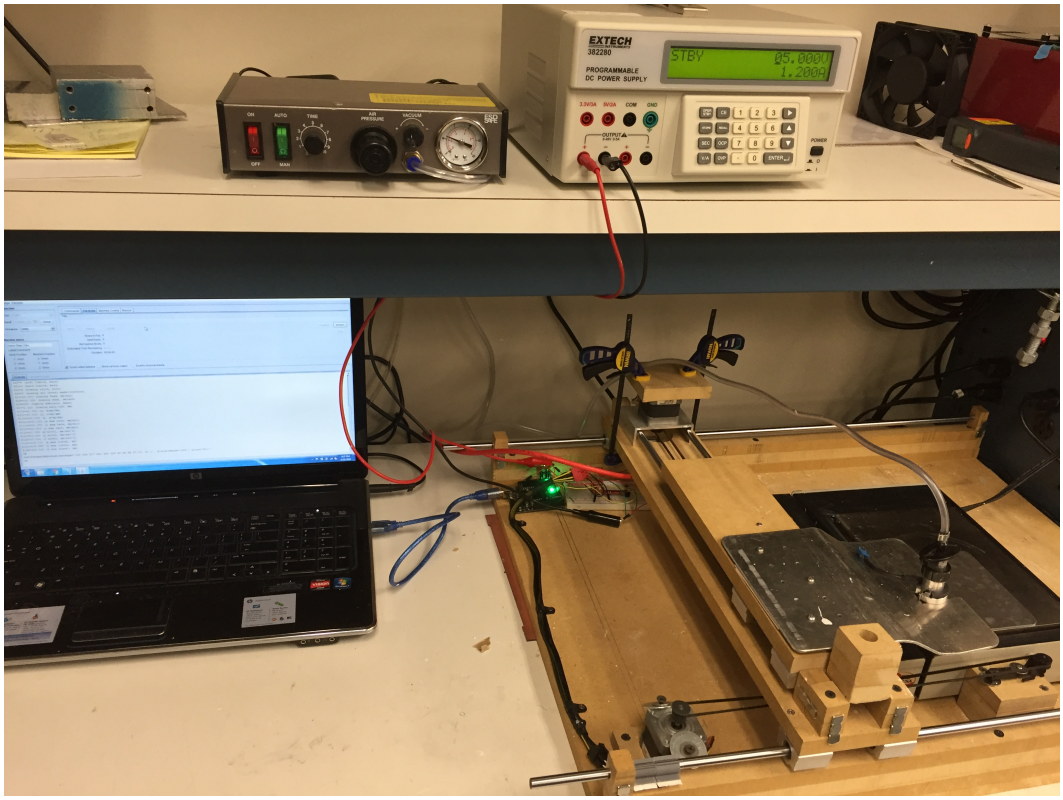

Figure 3.2: Fabricated 3D Printer

3.2 Ring Resonator

In order to characterize the quality of the printed Hereaus material, an RF device had to be designed and tested. The purpose of this device was to show the technology's ability to create complex, multi-layer devices while proving the feasibility for high frequency applications. A weakly-coupled ring resonator was selected then designed, simulated, and tested.

For nearly half a century, microstrip ring resonators have been used to measure the effective dielectric constant of substrates [20]. While these devices can be used to accurately measure important material information, ring resonators have also been used in filters, oscillators, mixers, and antennas [21]. Not only is this a proven RF device, it allows the printer to be tested in both dimensions simultaneous due to

the curved edges of the ring.

Figure 3.3 illustrates the geometry of a typical ring resonator from the top-side as well as a side angle. The coupling occurs in the region between microstrip feed and the ring. In Figure 3.3, the blue lines represent an illustration of the electric field on on the ring resonator and the green lines the electric field distribution around the open circuit termination of the microstrip feed lines. These lines overlap in the coupling gap region allowing energy to be transfer between the microstrip feed line and the ring resonator.

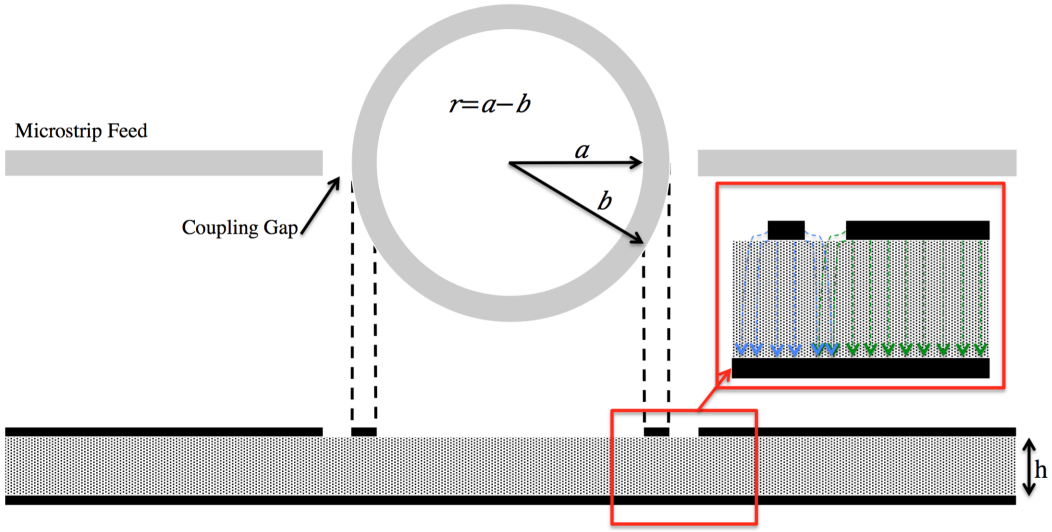

Figure 3.3: Illustration of the ring resonator along with the electric field distribution in the coupling region

Using the terms represented in Figure 3.3 the radius of a ring resonator can be described using

$$2\pi r = n\lambda_g \tag{3.1}$$

where, r is the mean radius of the ring, n is the mode number, λ_g is the guided wavelength. Furthermore, the resonant frequency can be calculated using

$$f_o = \frac{nc}{2\pi r\sqrt{\epsilon_{reff}}} \tag{3.2}$$

where, f_o is the resonant frequency, c is the speed of light, and ϵ_{reff} is the effective relative dielectric constant.

The ring resonator was designed using the above equations. Since the resonant frequency location was not critical, the radius was the chosen based on the size of the purchased alumina sheets, which were 25 mm wide, 48 mm long, and 25 mil thick. By choosing a radius of 5 mm, there would be sufficient distance from the resonator to the edge of the substrate. Based on this radius and the material having an effective dielectric of approximately 6.5 the device should have a resonant frequency of 3.743 GHz. While calculated frequency will be close to the simulated frequency, it will not be exact due to ϵ_{reff} varying with frequency.

Once the theoretical device was designed it was simulated using Ansys HFSS. Figure 3.4 shows the model used to simulate the ring resonator which includes the microstrip lines as well as the CPW feed used to measure the device. The resonant frequency according to simulation is 3.759 GHz which is less than a half a percent higher than the theoretical resonant frequency. HFSS is also used to verify the mode by plotting the field distribution on the ring to ensure it was in fact resonating and there wasn't an error in simulation. The electric field distribution of the first mode of the resonator can be seen in Figure 3.5.

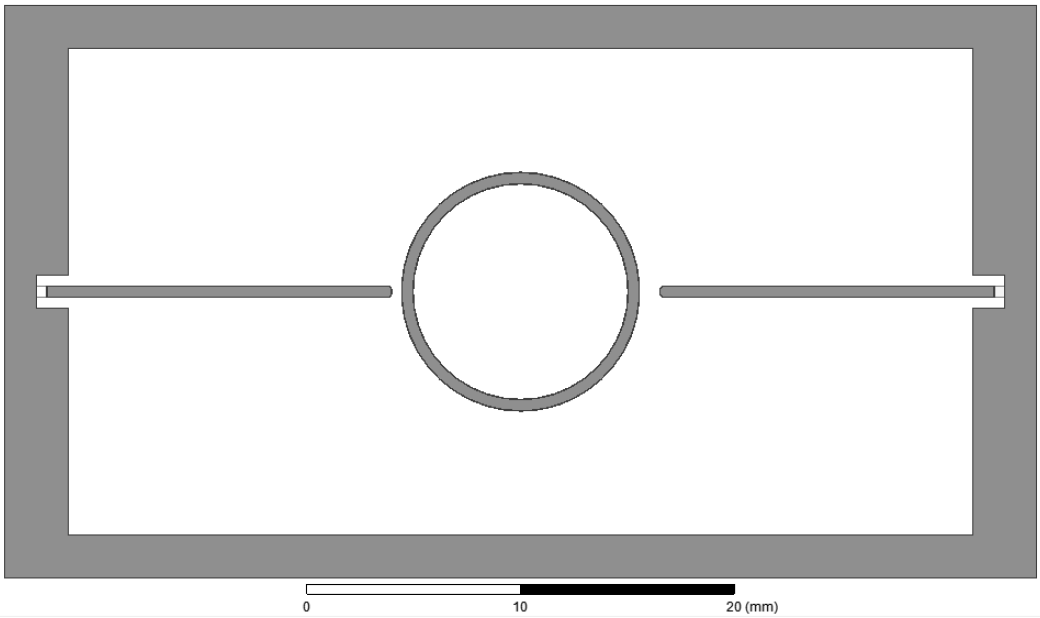

Figure 3.4: HFSS simulation model

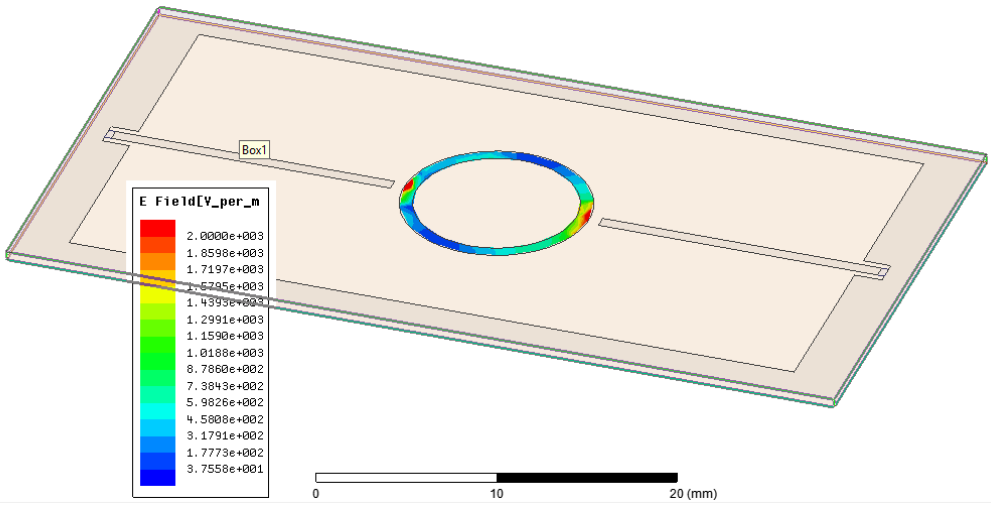

Figure 3.5: First resonant mode electric field distribution

In order for the resonator to be weakly coupled, the microstrip feed lines had to be placed far enough away to limit the about of energy transferred to the resonator. A gap of approximately 600 μm would allow the resonator to couple enough energy

to resonate but not enough to significant effect the loaded Q. Figure 3.6 shows the frequency response of the simulated device of the first resonant mode.

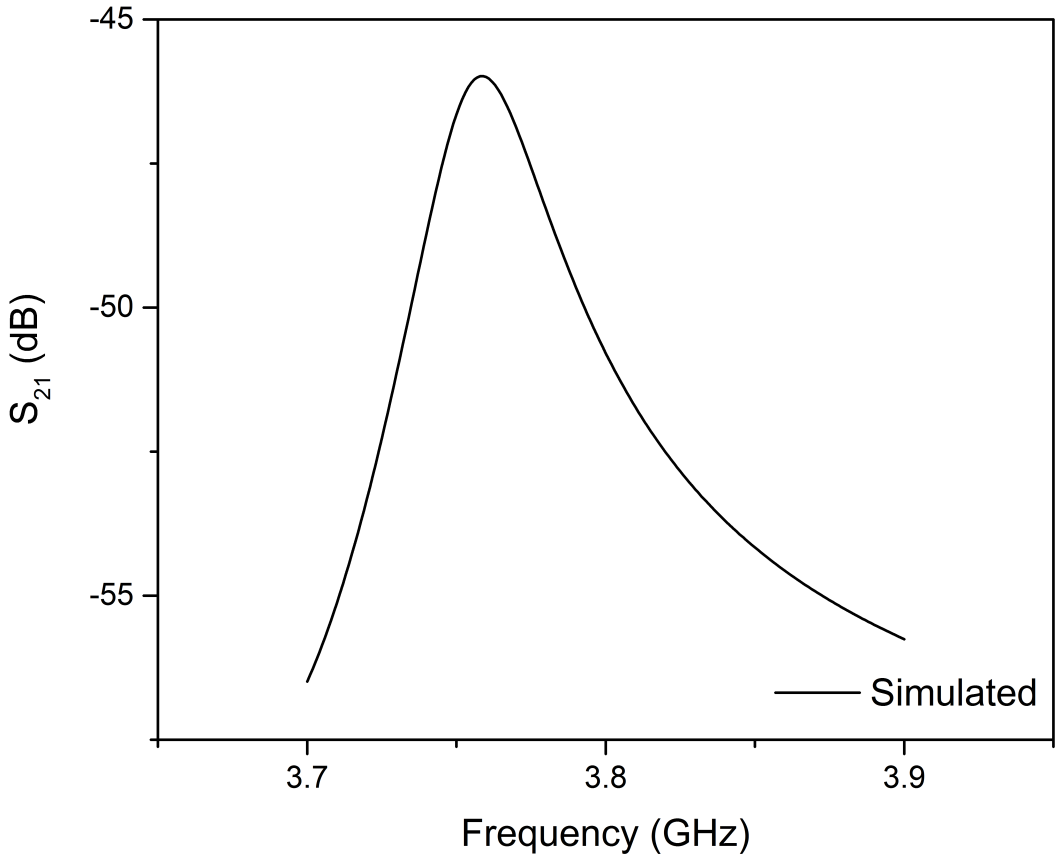

Figure 3.6: Simulated frequency response of ring resonator

The design phase consisted mainly of preparing the device to be built with the 3D printer. Based on the results from HFSS simulations as well as the printer's performance, successfully device fabrication should be achievable.

4 Measurement & Analysis

With the objective of creating a process to additive manufacture microwave devices, a functioning RF device had to be realized. As mentioned, a ring resonator was fabricated and in this section the results are presented.

4.1 Lithography-defined ring resonator

Prior to attempting to print the ring resonator with the printer, the design was fabricated using photolithography, a common subtractive manufacturing technique for precise microwave devices. Figure 4.1 shows the fabricated device as well as the device being measured using a probe station along with a set ground-signal-ground 1000 μm probes. In addition to the probe station, an Agilent Performance Network Analyzer (PNA) was used in conjunction with WinCal to capture the scattering parameters. To insure an accurate measurement, a calibration was done using SOLT references on an impedance standard substrate. The measured results are presented in Figure 4.2.

In measuring the device, copper tape was used to connect the top ground, which is used to connect to the PNA, to the bottom ground plane. This is important due to the transition from CPW feed to microstrip and the microstrip lines. Without the grounds being connected the response would not be as expected due to the microstrip line not having a ground plane.

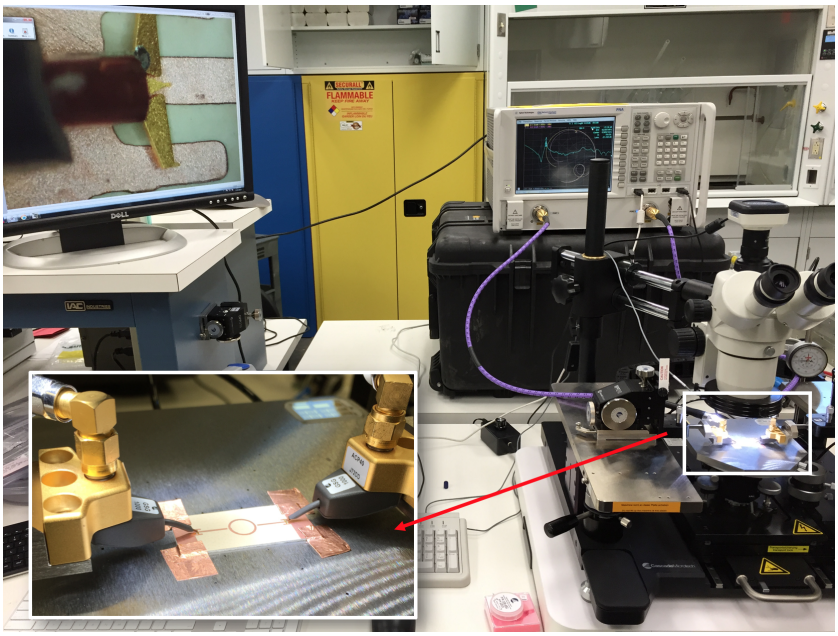

Figure 4.1: Measurement setup of initial ring resonator

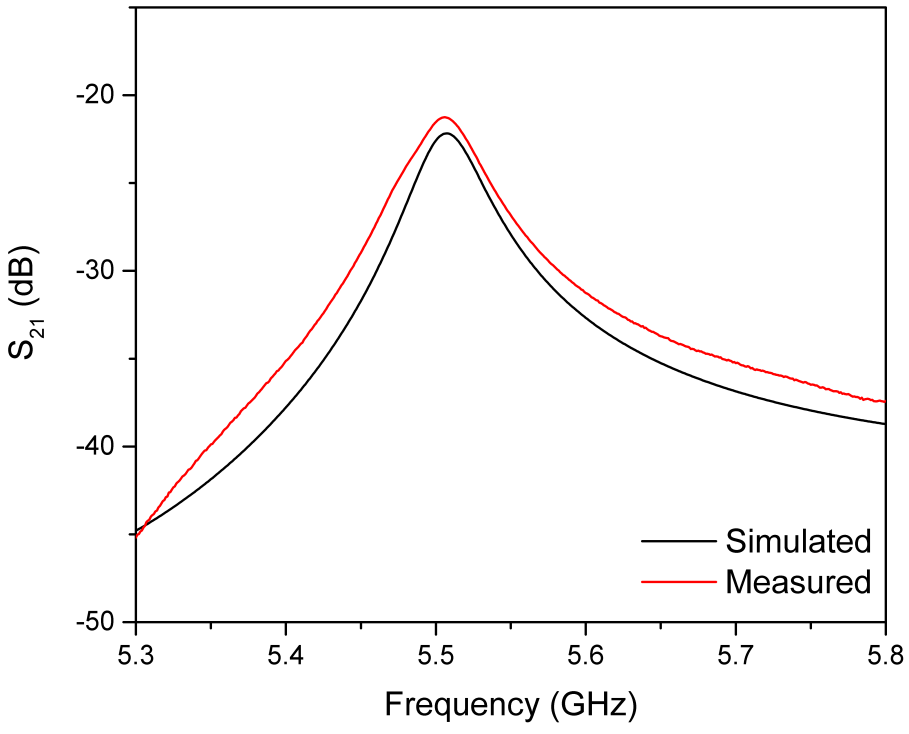

Figure 4.2: Simulated and measured insertion loss of lithography resonator

4.2 Thick-film silver ring resonator

Once the design was verified using the above subtractive manufacturing technique, the next step was to fabricate a ring resonator with additive manufacturing techniques. In the first experiment, only the conductive layer was printed. The printer described in Section 3.1 was used to dispense the conductive layer onto a 25-mil alumina sheet. The device was fired and the measured with the same setup used to measure the previous resonator. The printed resonator on alumina can be seen in Figure 4.3.

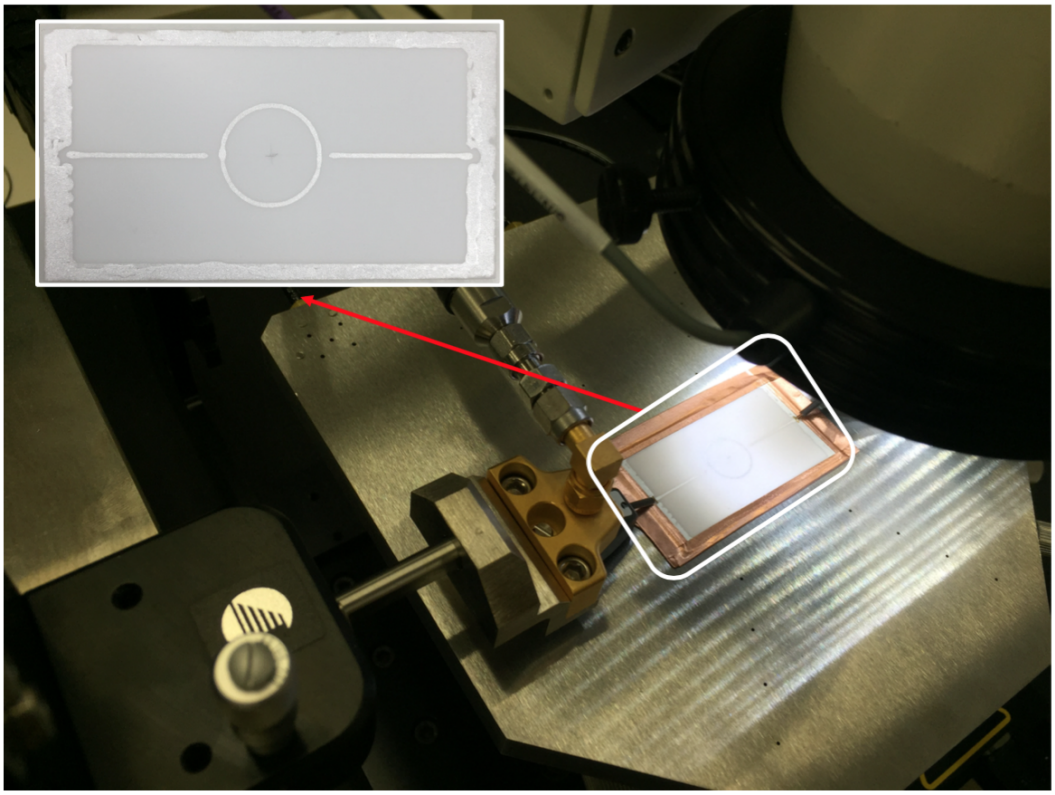

Figure 4.3: Printed silver ring resonator testing

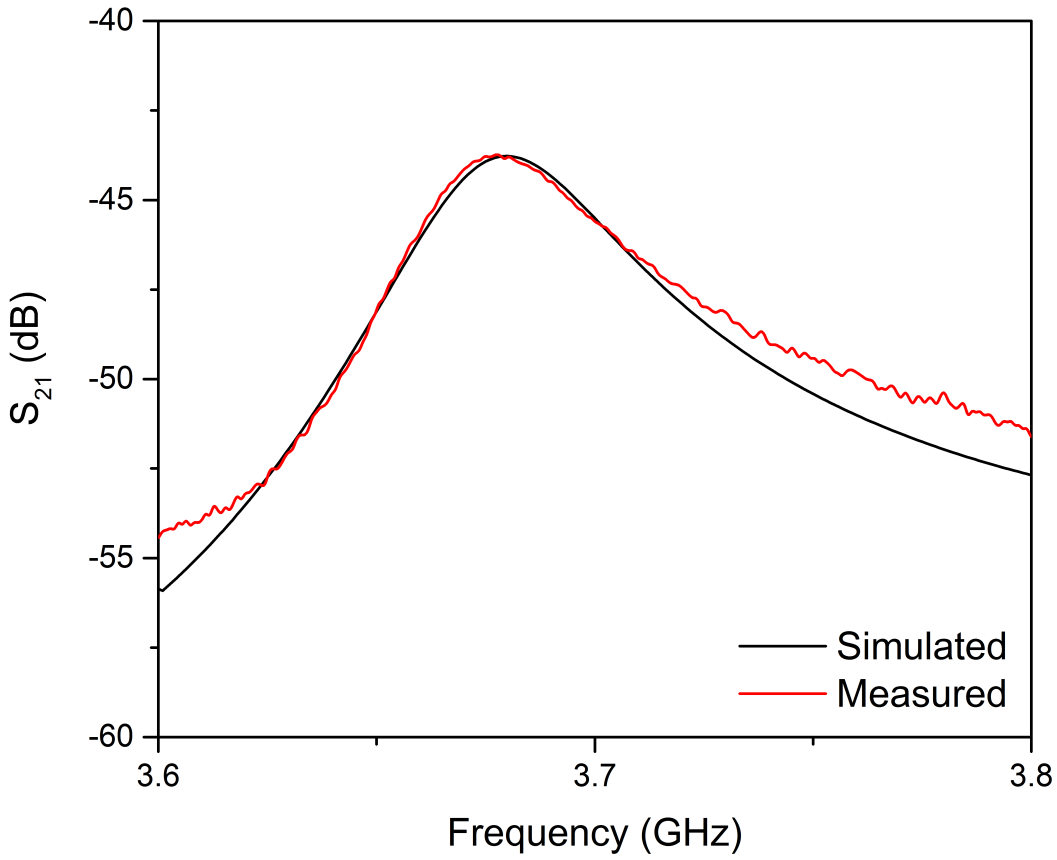

Figure 4.4: Thick-film device frequency response

4.3 Printed LTCC ring resonator

The last device that was measured was a ring resonator where not only the silver layer was printed, but also the ceramic layer. This device adds significant value to the claim that LTCC can be additively manufactured. The ceramic layer was printed from a ceramic slurry composed of LTCC specific ceramic powder. Contrary to the previous fabricated devices that were tested, this device is composed solely of LTCC materials that were additively manufactured. As a result of printing limitations, the thickness of the ceramic is around 25% thinner than the alumina sheet leading to a different RF response. The device can be seen in Figure 4.5.

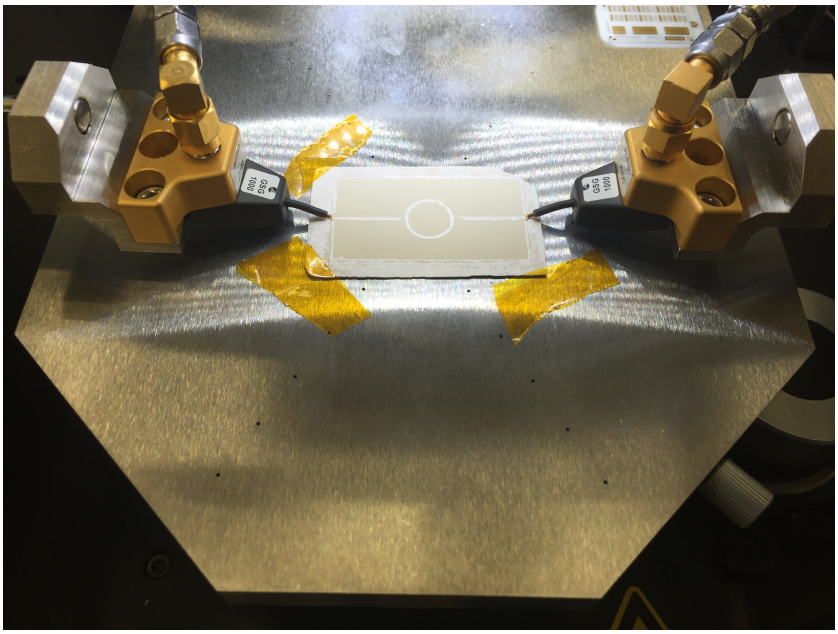

Figure 4.5: Printed LTCC ring resonator

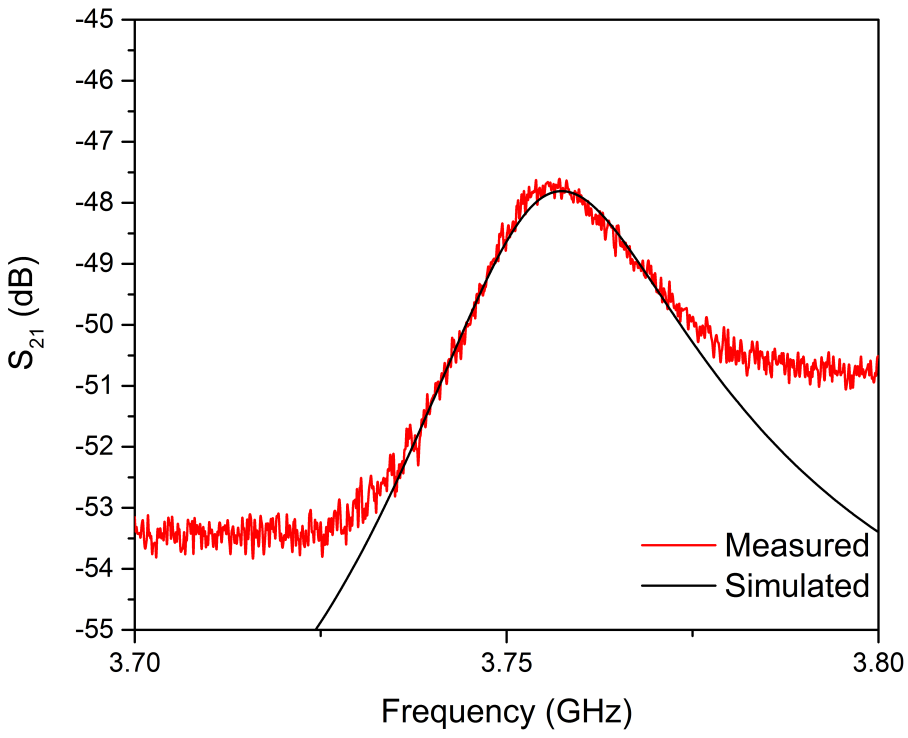

Figure 4.6: LTCC device frequency response

4.4 Measurement Analysis

The ring resonators were analysed based on how well the fabricated devices correlated with the simulations. The center frequency of the resonator along with the quality factor,Q were compared. The higher the Q, the lower the loss of a resonant circuit. Resonator losses can be attributed to conductor losses, dielectric losses or radiation losses. Loaded Q, Q_L, is easily extracted from measurements using (4.1) where f_u and f_l are the 3-dB lower than f_c.

$$Q_L = \frac{1}{FBW} = \frac{1}{\frac{f_c}{f_u - f_l}} = \frac{f_u - f_l}{f_c} \tag{4.1}$$

A more relevant parameter is unloaded quality factor, Q_U, and can be found using (4.2) By the resonator being weakly coupled, the magnitude of S_{21} is relative small. As a result, the Q_L and Q_U are nearly equal.

$$Q_U = \frac{Q_L}{1 - |S_{21}|} \tag{4.2}$$

The quality factor was also used to refine the simulation of the ring resonators. As mentioned previously, the simulated Q was high than the measured. In order to reduce the variation between the simulation and the fabricated device, the simulation was modified to more accurately represent the fabricated device. This included adding the measured conductor thickness to the simulation as well as rounded edges of the printed lines. The fabricated device was measured using an Alpha Step profilometer. Once the 3D model more accurately represented the fabricated device, the conductivity of the silver was reduced until the quality factor agreed with the quality factor of the fabricated device.

The simulated quality factors along with the measured quality factors are presented in Table 4.1. Not only do the quality factors of the simulated device agree

with the fabricate one, the resonant frequencies also agree.

Table 4.1: Summary of results

Fabrication Technique	Radius (mm)	Theoretical Resonant Frequency (GHz)	Simulated Resonant Frequency (GHz)	Measured Resonant Frequency (GHz)	Simulated Q	Measured Q
Lithography	3.41	5.535	5.507	5.506	118	104
Thick-Film	5.29	3.5386	3.68	3.6766	66	66
LTCC	5.02	3.7284	3.759	3.755	103	103

The effective conductivity of the silver is 9×10^6 S/m. This was determined using the sample created on alumina due to the material having known material properties. The material used in simulation was alumina with a dielectric constant of 9.4 and a loss tangent of 0.007. The effective conductivity also takes into account parasitic effects such as surface roughness of the material. By mirroring the 3D model in HFSS to the fabricated device, the measured and simulated quality factory agree within less than a tenth of a percent when the conductivity of the silver is set to 9×10^6 S/m. According to the datasheet of the printed silver, the conductivity is 33×10^6 S/m. The difference between the datasheet conductivity and the effective conductivity is attributed to the surface roughness of the printed material. Another source of loss in the device is due to the dielectric layers. This loss is due to the dissipation of energy in the dielectric and quantified by the loss tangent, $\tan \delta$. In order to determine the loss tangent of the ceramic material used, an HFSS simulation was used in conjunction with the effective conductivity of the printed silver. Similar to the the method used to determine the conductivity of the silver, the loss tangent was determined by adjusting simulation until the quality factors agreed. The loss tangent was determined to be 0.001.

While this process can be used to determine the losses of unknown materials, at least one of the materials must have known properties. In this case, the known

material was alumina. Using the sample that was composed of printed silver and alumina, the effective conductivity of the silver can be determined. By knowing the effective conductivity of the silver, the loss tangent of printing ceramic could be found. Although this method can be used to determine both conductivity and loss tangent it relies heavily on the measurement of the fabricated device as well as the known material properties.

5 Conclusions

The ability to additive manufacturing low-temperature co-fired ceramic would be an excellent resource for researchers allowing them to test designs by rapidly prototyping their devices quicker and cheaper than ever before. The goal of the presented research was to prove this process was possible by building and testing microwave devices.

Based on the devices that were fabricated, it can be stated LTCC can be additively manufactured. The measured results agreed well with simulations based on center frequencies and quality factors. Not only can the proposed process be used to additively manufacture thick-film devices but it can also be used for LTCC devices. Prior to this research, no known LTCC devices have been created using additive manufacturing.

The progress presented in this document provides proof that additive manufacturing at LTCC material sets is no longer impossible. This was verified by the fabrication of a ring resonator. This work has combined the desired features of LTCC along with the ability to rapidly prototype due to using additive manufacturing techniques.

5.1 Improvements and Future Work

Although the results of the research are promising, further developments are necessary before the printer can fabricate a device without complications. The main improvement that can be made is a higher quality printer, such as a nScrypt. This improvement would increase the dimensional resolution from greater than 50 μm to less than 10 μm. Furthermore, the nScrypt offers improvements in dispensing over the current needle dispensing methods.

The existing printer could also be used in the future if a few improvements were

made. First, the z-axis of the platform needs to be more uniform. This would allow for thinner, more uniform layers to be printed. Furthermore, the software used to control the printer would need to be upgraded. Current fabrication requires manually creating the file that instructs the printer where to go. This would not be user-friendly for complex, multi-layer devices.

Common to many additively manufactured techniques, the surface roughness of the fabricated parts could also be improved. Surface roughness can cause increased losses versus a smooth surface of the same material.

Another improvement that would allow for easier printing would be finding a printing platform that could withstand the high sintering temperatures. Current methods require the part to be removed from the building platform and placed on a piece of ceramic for firing. While this method is functional, it adds an extra step to the user and is another point of failure in the process. Due to the tape being dry, it is extremely fragile and can easily be cracked. One possible solution to this is printing on pre-manufactured green tape.

Lastly, in order to expand the process to allow for more complex designs, additional materials need to be tested and characterized. Currently only ceramic and silver have been investigated. By additional materials, this process can be expanded to fabricated a variety of sensors and other useful devices.

References

[1] T. Eastman and A. Cook, "Direct write electronics-thick films on LTCC," in *International Symposium on Microelectronics*, International Microelectronics Assembly and Packaging Society, vol. 2014, 2014, pp. 000 893–000 897.

[2] H. Birol, "Fabrication of low temperature co-fired ceramic (LTCC)-based sensor and micro-fluidic structures," 2007.

[3] K. Equipment. (2016). MLCC, MLCI, MLCV, LTCC,... electronic manufacturing equipment, [Online]. Available: `http://www.keko-equipment.com/PRODUCTS.php`.

[4] Dupont, "Greentape design and layout guidelines," 2009.

[5] C. Hull, *Apparatus for production of three-dimensional objects by stereolithography*, US Patent 4,575,330, Mar. 1986. [Online]. Available: `https://www.google.com/patents/US4575330`.

[6] A. Standard, "F2792. 2012. standard terminology for additive manufacturing technologies," *ASTM F2792-10e1*, 2012.

[7] L. U. AMRG. (2016). The 7 categories of additive manufacturing, [Online]. Available: `http://www.lboro.ac.uk/research/amrg/about/the7categoriesofadditivemanufacturing/`.

[8] Y. Huang, X. Gong, S. Hajela, and W. J. Chappell, "Layer-by-layer stereolithography of three-dimensional antennas," in *Antennas and Propagation Society International Symposium, 2005 IEEE*, IEEE, vol. 1, 2005, pp. 276–279.

[9] X. Gong, A. Margomenos, B. Liu, W. J. Chappell, and L. P. Katehi, "High-Q evanescent-mode filters using silicon micromachining and polymer stereolithography (SL) processing," in *Microwave Symposium Digest, 2004 IEEE MTT-S International*, IEEE, vol. 2, 2004, pp. 433–436.

[10] E. A. Rojas-Nastrucci, T. Weller, V. Lopez Aida, F. Cai, and J. Papapolymerou, "A study on 3D-printed coplanar waveguide with meshed and finite ground planes," in *Wireless and Microwave Technology Conference (WAMICON), 2014 IEEE 15th Annual*, IEEE, 2014, pp. 1–3.

[11] I. T. Nassar and T. M. Weller, "An electrically-small, 3-D cube antenna fabricated with additive manufacturing," in *Power Amplifiers for Wireless and Radio Applications (PAWR), 2013 IEEE Topical Conference on*, IEEE, 2013, pp. 91–93.

[12] I. Nassar, H. Tsang, and T. Weller, "3D printed wideband harmonic transceiver for embedded passive wireless monitoring," *Electronics Letters*, vol. 50, no. 22, pp. 1609–1611, 2014.

[13] K. F. Brakora, J. Halloran, and K. Sarabandi, "Design of 3-D monolithic mmw antennas using ceramic stereolithography," *Antennas and Propagation, IEEE Transactions on*, vol. 55, no. 3, pp. 790–797, 2007.

[14] A. Buerkle, K. F. Brakora, and K. Sarabandi, "Fabrication of a DRA array using ceramic stereolithography," *Antennas and Wireless Propagation Letters, IEEE*, vol. 5, no. 1, pp. 479–482, 2006.

[15] B. Liu, X. Gong, and W. J. Chappell, "Applications of layer-by-layer polymer stereolithography for three-dimensional high-frequency components," *Microwave Theory and Techniques, IEEE Transactions on*, vol. 52, no. 11, pp. 2567–2575, 2004.

[16] K. C. Wu, "Parametric study and optimization of ceramic stereolithography," PhD thesis, University of Michigan, Ann Arbor, MI, 2005.

[17] M. D. Benge, R. C. Huck, and H. H. Sigmarsson, "X-band performance of three-dimensional, selectively laser sintered waveguides," in *Antennas and Propagation Society International Symposium (APSURSI), 2014 IEEE*, IEEE, 2014, pp. 13–14.

[18] X. Chen, K. Church, A. Karbasi, and W. K. Jones, "Micro-dispense direct printing for thermal management structure using LTCC," *Additional Papers and Presentations*, vol. 2013, no. CICMT, pp. 000 221–000 225, 2013.

[19] N. Arnal, T. Ketterl, Y. Vega, J. Stratton, C. Perkowski, P. Deffenbaugh, K. Church, and T. Weller, "3D multi-layer additive manufacturing of a 2.45 GHz RF front end," in *Microwave Symposium (IMS), 2015 IEEE MTT-S International*, IEEE, 2015, pp. 1–4.

[20] P. Troughton, "Measurement techniques in microstrip," *Electronics Letters*, vol. 5, no. 2, pp. 25–26, 1969.

[21] L.-H. Hsieh and K. Chang, "Equivalent lumped elements G, L, C, and unloaded Q's of closed-and open-loop ring resonators," *Microwave Theory and Techniques, IEEE Transactions on*, vol. 50, no. 2, pp. 453–460, 2002.

[22] R. C. Buchanan, *Ceramic materials for electronics*. CRC press, 2004, vol. 68.

Appendix A Fabrication Instructions

In this section includes instructions that can be followed by later people to recreate multi-layer ceramic materials using the above practices.

Table A.1: Outline of fabrication process

Step	Description	Materials Required	Equiptment Required
1	Prepare slurry	X-200W, SR238, CC55	Scale, jar, ball mill(optional)
2	Prepare silver	Silver, thinner	jar
3	Prepare Printing Platform	PTFE sheet, metal sheet, spray adhesive, isopropyl alcohol	N/A
4	Prepare G-Code Files	G-Code Files	N/A
5	Prepare Printer	N/A	Power Supply, Arduino
6	Print layer	Ceramic slurry, syringe, plunger, needle	Pneumatic dispenser
7	Vacuum layer (if ceramic)	N/A	Vacuum pump, vacuum chamber
8	Dry layer	N/A	Hot plate or oven
	Repeat steps 4-8 for each layer		

1. **Prepare Slurry**
   To prepare the slurry, reference the excel spreadsheet to determine the appropriated amount of X-200W, monomer, and dispersant that are needed. For simplicity the recipe found in table A.2 can be scaled and is based on the following parameters: the batch size is 20 cc, X-200W loading of 60%, and 2% dispersant. Using a scale, measure the appropriate amount of material and thoroughly mix the slurry. For easier mixing, only add approximately 80% of the ceramic powder, along with all of the monomer and dispersant; after

Table A.2: Example slurry recipe

Composition	wt, g	wt%	vol, cc	vol%
Ceramic	48.00	85.50%	12.00	60.00%
Monomer	7.18	12.79%	7.04	35.20%
Dispersant	0.96	1.71%	0.96	4.80%
Total	56.1	100.00%	20	100.00%

the slurry has become viscous continue adding and stirring the slurry until the desired amount of ceramic powder is added. In addition, zirconium oxide balls can be added to the mixture to aid in mixing. If the slurry is left for a period of time remixing will be required.

2. **Prepare silver** The silver mixture that is dispensed is composed of only two components: Heraeus TC2306 and the thinner. TC2306 is the Ag conductor paste and thinner is the thinning agent used to reduce the viscosity of the paste. In order to be able to dispense TC2306 it must first be thinned. This is done by adding the desired about of TC2306 to a small mixing jar. Next, add a drop of the thinner and mix thoroughly. If the material is still to thick, add another drop and repeat the process. Once the material is viscous enough to be able to dispense, transfer material to syringe for printing.

3. **Prepare Printing Platform** The layers are printing onto a platform where the layers are dried then removed. In order for the platform to be able to release the dried layer, a non-stick film is used. However, in order to eliminate the film from curling when heated, it should be adhered to a piece of metal. In previous cases, a 10 mil piece of Rogers 5880 was adhered to a sheet of metal.

   Care must also be taken to remove dried samples from the build platform. If the non-stick layer is damaged, it must be replaced. Furthermore the layer should be cleaned between uses to ensure contaminates are kept to a minimum.

4. **Prepare G-Code Files** The printer is operated based on G-code commands. A series of commands are compiled into a single .gcode file and uploaded to the printer. This .gcode file is created using text edit and saving the file as a .gcode instead of .txt. Figure A.1 is an example file that was used to print the ring resonator.

5. **Prepare Printer** The printer is composed of three parts, the platform including stepper motors, the controller, and a computer to operate the controller. The stepper motors are controlled using EasyDriver stepper motor drivers

```
G21
F100
G00 X-21.4075Y-11.6125
G04P1
G01 Y-1.0231
G01 X-22.9194
G01 Y1.0231
G01 X-21.4075
G01 Y11.6125
G01 X21.4075
G01 Y1.0231
G01 X22.9194
G01 Y-1.0231
G01 X21.4075
G01 Y-11.6125
G01 X-21.4075

G04P1
G00 X-6.0205Y0
G04P1
G01 X-21.6193
G04P1
G00 X6.0205Y0
G04P1
G01 X21.6193
G04P1
G00 X-5.2575Y0
G04P1
G02 X-5.2575Y0I5.2575J0
```

Figure A.1: Example G-Code commands used to fabricate ring resonator

along with a DC power supply. The controller is an Arduino Uno loaded with grbl, an open-source g-code interpreter. This low-cost solution allows the printer to be controlled using another open-source application, Universal-G-Code-Sender.

6. **Print layer** To print a layer, first turn on the power supply and make the appropriate connections. Next using Universal-G-Code-Sender, establish a connection with the Arduino at 115200 baud. Once the connection has been established, the printer can be controlled using the program. Upload the .gcode file created in the previous step. Next, with the DC power supply output off, move the printer stage to the desired location. This will be the origin of the printer. To set the z-axis to the desired height, using weights to lower the height. Finally turn on the power supply and send the file to the Arduino.

7. **Vacuum layer** In order to prevent bubbles in printed layers, each layer should be vacuumed prior to being dried. This can be done by placing the build platform into the vacuum chamber and allowing it to remain there until all bubbles have excaped.

8. **Dry Layer** Silver layers should be dried at no more than 80^{o}C and ceramic layers should be dried at 120^{o}C.

Appendix B Experiment Details

Table B.1: Overview of included experiments

Experiment Category	Related Experiments	Results
Slurry	1. Initial slurry mixture 2. Impact of CC55 6. Mixture rate variation 23. Increase ceramic loading	1. Uniform mixture was not possible 2. Ceramic dispersant is required 6. Mixture rate does not effect settling 23. Eliminated sintering cracking in multi-material builds
Ceramic	8. Multi-layer ceramic build 9. Reduction in layer thickness 10. Sintering stacked, dry layers 12. Ceramic drying temperatures 16. Air bubble causes 18. Ceramic Printing 21. Alternative drying methods	8. Ceramic layers adhere together 9. Cracking reduced but warping occurred 10. Pre-dryed layers do not adhere during sintering 12. Ceramic should be dried at 125°C 16. Vacuuming prior to drying elminated air bubbles 18. Processes determinted to print ceramic layer 21. The drying divot could be removed but required non-traditional methods.
Silver	5. Wet silver & Ceramic Interaction 19. Ceramic & Silver Interaction (Post dried) 20. Silver dry temerature	5. Layers must be dry before dispensing another layer 19. Cracking occurs when silver layers are printed on top of printer ceramic layers 20. Silver must be dried at 80°C
Build Platform	4. Teflon coated platform 7. PTFE sheet platform 11. Photoresist coated platform 22. Copper platform	4. The Teflon coating was too thin plyable 7. 10 mil PTFE sheet adhered to metal worked well 11. Photoresist did not work well for printing 22. Not a viable option due to copper oxide
Printer Fabrication	14. Initial printing 15. High-resolution printing	14. Stepper motor resolution not adiquate 15. Improved resolution to 19 steps/mm
Design Verification	3. Lithography Design 13. DC testing 17. Ring resonator on alumina 24. Ring resonator on X-200W	3. Design verified using etched resonator on TMM10i 13. The embedded trace was conductive 17. Design verified by printing ring on alumina sheet 24. Design build and tested on LTCC materials

1. **Initial ceramic slurry**
   Goal: Create a slurry using known good recipe using X-200W powder and SR238 monomer. The dispersant was deliberately withheld due to lack of availability.
   Description: The initial four months of research was spent investigating mixing the slurry without the use of a dispersant. This was due largely to unavailability of a ceramic dispersant. Variquat has discontinued CC55 as well as its successor CC59. The main obstacle during this period was the material cracking during the co-fire stage. Several causes were proposed to be the culprit of the cracking: inadequate loading of ceramic in the slurry, adhesion of the slurry to the carrier alumina sheet, increasing the temperature too rapid during sintering, and the absents of a dispersant.
   Results: Figure B.1 shows the cracking that was common in post-sintered ceramic that was fired without a dispersant. In addition to the cracking, the

surface quality was rough and would not be well suited for RF applications.

(a) Post-fired

(b) Post-fired

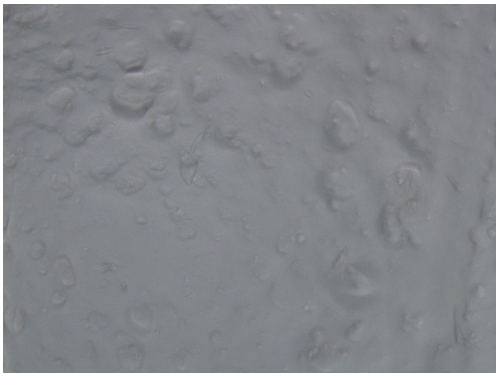

(c) Post-fired Microscope

(d) Pre-fired, dryed on Kapton

Figure B.1: Coupons without ceramic dispersant

2. **Addition of dispersant to ceramic slurry**
   Goal:Determine impact of dispersant on the slurry
   Description: After numerous experiments varying the mixing concentrations of ceramic in the slurry, it was determined that a dispersant would be required to create a uniformly mixed ceramic slurry. In the initial experiment with the dispersant, the appropriate amount of ceramic and monomer were added but the dispersant was intentionally withheld. After the physical properties of the mixture were recorded, the dispersant was added.
   Results: The addition of the dispersant to the ceramic mixture transformed a clumpy powder into a viscous slurry that was able to be uniformly mixed. It is also worth mentioning that after the slurry sat undisturbed for several hours, it would begin to settle. The ceramic powder would sink to the bottom and the top would become clear. The mixture could easily be mixed back to its uniform state.

3. **Lithography device verification**
   Goal: Verify proposed design functionality before attempting to build using additive manufacturing techniques
   Description:The test device was created on Rogers TMM10i substrate to closely represent the ceramic material that would be later printed. Using traditional board manufacturing lithography processes, the device was etched. Once the device was successfully fabricated it was measured using a Cascade MicroTech probe station and an Agilent VNA.
   Results: The design was verified to function as expected based on the measurements taken from the VNA of the test device that was creating using lithography techniques. Measurement results of this resonator can be found in Section 4.

4. **Teflon wrapped building platform**
   Goal: Prevent wet slurry from adhering to build platform by using a non-stick material such as Teflon
   Description: In order to prevent the slurry from adhering during the drying stage to the building platform, a thin teflon sheet was wrapped around a sheet of copper.
   Results: While the Teflon sheet did provide a nonstick surface for the slurry to dry, it did not have any rigidity and would easily slide around. This was problematic when trying to remove the fragile dried slurry because the backing would move causing the dried material to crack.

5. **Wet silver & ceramic Interaction**
   Goal: Determine interaction between wet/dry silver and wet/dry ceramic
   Description: In order to properly print stacked ceramic and silver layers, the interaction of the two materials must be known. For example, if the slurry must be completely dry prior to printing the silver. In order to determine this, two tests were conducted. First, a silver line was printed onto an alumina sheet and while the silver trace was still wet, a slurry trace was applied parallel, touching the silver trace. The two traces where then dried and inspected. The second test involved the two previous traces as well as a third ceramic trace. The third trace was applied on the other side of the dried silver trace as well as creating a ceramic bridge connecting two two outside ceramic traces.
   Results: Based on the results from the first test, ceramic layers should not be printed touching un-dried silver layers. The silver bled into the ceramic making it no longer white, but the ceramic didn't appear to blend into the silver. However, based on the second test, once the silver has dried, additional ceramic layers can be added. If the silver is not completely dry, do not print ceramic to prevent unwanted mixing of traces and layers. Figure B.2 shows

the fired sample from this experiment.

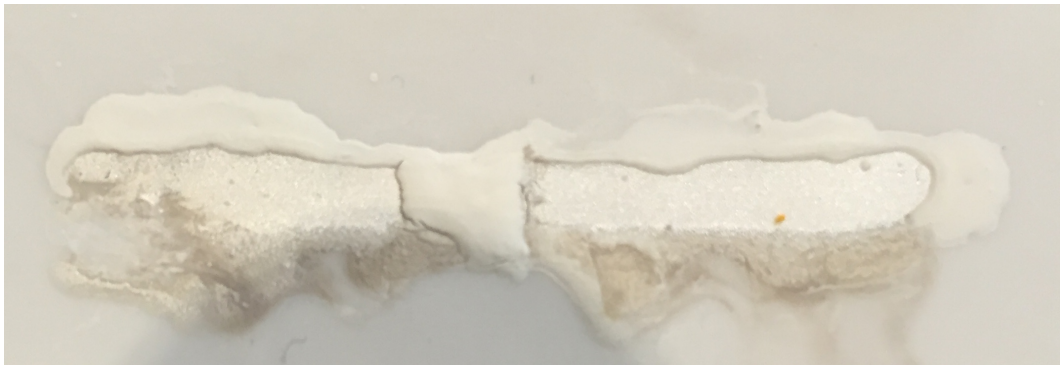

Figure B.2: Fired sample illustrating importance of drying between layers

6. **Slurry mixture rate variation**
   Goal: Prevent slurry from settling by controlling mixture rate
   Description: As previously mentioned in Experiment 1, the slurry would separate if undisturbed for several hours. This occurrence was most noticeable when the material was left unused for several days. The cause of the settling was thought to be the result of not correctly mixing the slurry. Instead of mixing the ceramic in incremental stages as recommended by the University of Michigan recipe, it was added all at once. To determine if this was the cause of the settling, the slurry was mixed according to the recommendation. The reason this was not done initially is that it takes approximately eight hours to mix per recommendations.
   Results: The slurry that was mixed per recommendations exhibited the identical settling that occurred in the rapidly mixed slurry. Future slurry mixing will be completed by adding all the materials at once except when loading in increased to 60% as in Experiment 23.

7. **PTFE building platform**
   Goal: Prevent wet slurry from adhering to build platform by using an alternative to thin Teflon sheets
   Description: Due to the thin Teflon sheet bunching up when removing the dried slurry, alternative non-stick materials were investigated. The material that was proposed as a replacement was Rogers 5880 board material. This was chosen due to being PTFE based as well as availability. PTFE is the non-copyrighted name of Teflon. Several layer thickness were investigated including 10, 20, and 125 mil.
   Results: The initial board material tested was 10 mil thick. The non-stick

properties were promising but had a significant physical complication. As the material was heated it would begin to deform and curl, and as a result slurry dried on this platform would also be deformed. To attempt to reduce the bowing the board material, the thickness was increased to 20 mil but the complication reoccurred. The other readily available thickness was 125 mil. While this material did not bow when heated, it did not conduct heat very well and the drying times were drastically increased. To achieve the non-stick property and maintain adequate heat transfer, a 10 mil layer of Rogers 5880 was adhered to a sheet of metal. The thin layer of PTFE offered the non-stick feature while the metal sheet offered rigidity and conductivity.

8. **Multi-layer ceramic build**
   Goal: Verify single layer building processes are functional for multiple ceramic layers
   Description: Up until this point, only single layers had been printed. The goal was to extend the findings to multi-layer ceramic pieces. This was done by creating a coupon that contained three layers. Each layer was dried using a hot plate at 125^{o}C prior to printing another layer. Once all the layers were dried the multi-layer piece was co-fired.
   Results: The diameter of the test piece was similar to the size of a dime. Each of the three layers adhered to the neighboring layers during drying. In addition to the three layers, a small drop of slurry was placed as a ball onto of a layer of dried ceramic. The post fired sample did not have any separation between layers and didn't have any external defects such as cracking visible. The only visible interface between sintered layers is the presents of air bubbles.

9. **Reduction in layer thickness**
   Goal: Prevent cracking during the drying and sintering stages by reducing layer thickness
   Description: In previous experiments, the ceramic layers would commonly crack during the drying of the layer. The cracking occurs once the coupon has nearly dried. This is because as the slurry dries, it shrinks slightly. The location of where the drying completes a small divot is created. This divot is the location where the crack originates. The goal is to try and minimize this defect by reducing layer thickness. No other changes were made to the experiment setup other than the thickness of the ceramic layer. Once the layers were dried they were removed from the building platform and fired.
   Results: The piece did not crack during drying but it did warp slightly. The warping was increased during the sintering and the piece also cracked. The cause of the cracking was unknown. Warping was likely the result of the thin

single layer curling during sintering. .

10. **Adhesion of sintered stacked, dry layers**
    Goal: Determine if two dried layers will adhere to one another if each layer is dried separately then stacked on-top on on another and sintered
    Description: In earlier experiments, layers were verified to adhere if one of the layers was wet when they were joined. In this experiment, the joining layers were both dry before being in contact with each other. The two layers were stacked and co-fired.
    Results: The two, flat ceramic pieces were still separable after they were sintered. As a result it can be stated that two separately dried ceramic sheets will not sinter to one another if they are not joined before they are dry or at least one of the layers has to be wet.

11. **Photoresist coated building platform**
    Goal: Print ceramic layer on photoresist then dissolve photoresist layer
    Description: Instead of using a PTFE building platform, a sheet of metal was covered in photoresist. The purpose of this was to allow a ceramic layer to be built on a layer of photoresist and after the build was complete, dissolve the photoresist away using sodium carbonate.
    Results: The green photoresist turned blue during the drying of the slurry. Furthermore the sodium carbonate also leached into the dry ceramic causing it to break down.

12. **Ceramic drying temperatures**
    Goal: Find the optimum drying temperature taking into consideration the drying duration as well as material quality post dried
    Description: Since the objective is to create a building process where multiple layers of ceramic can be printed, the duration each layer must be dried between layer prints must be known. To determine the optimum drying temperature, the same size coupon was printed and dried at different temperatures on a hot plate. The tested temperatures were 75^{o}C, 100^{o}C, 125^{o}C, and 150^{o}C and dry time as well presents of bubbles in the dried material as well as any other observable defect were recorded.
    Results: The first temperature tested was 75^{o}C and after 10 minutes of no physical change the temperature was increased to 100^{o}C where it took an addition 55 minutes to dry completely. At 125^{o}C, the material took 15 minutes to dry and only 10 minutes to dry at 150^{o}C but had noticeable more bubble on the bottom side of the material. Due to the drying time of 125^{o}C being only five minutes longer and the improvement in material quality, future builds will be dried at 125^{o}C.

13. **DC testing**
    Goal: Verify buried silver trace conductivity by creating multi-layer ceramic-silver-ceramic device that can be tested using multimeter
    Description: In order to verify the functionality of buried silver in ceramic layers, a device was created that contained a buried silver trace between two ceramic layers. This device as built by printing a ceramic layer onto a building platform and drying the ceramic layer. Once the ceramic layer was dry, a silver trace was dispensed around the board with the ends at the edges of the board. After the silver was dry, another layer of ceramic was applied to embed the silver trace, but left the ends of the trace exposed in order to measure the resistance of the line. Once the final layer of ceramic was dry, the piece was placed into the oven and sintered.
    Results: The resulting co-fired piece was measured using a Keithley multimeter and a pair of DC probes. The measured resistance of the embedded line was 76.9 mΩ

Figure B.3: Post-fired DC test sample

14. **Initial printing**
    Goal: Print basic geometries using fabricated printer
    Description: This was the first experiment that was conducted using the fabricated printer. The goal of this experiment was to determine if the printer would have the ability to print at a high enough resolution to be able to fabricate microwave devices. In order to test the printer, basic commands were instructed and the results observed. For example, move the print head at a certain rate.
    Results: The resolution of the ink-jet printer stepper motors are not adequate to print microwave devices. This was concluded by instructing the printer to move in the x-axis at a constant, slow rate to simulate printing ceramic or silver. The movements made were jumpy and the resolution was only about half a millimeter. From some applications this would be acceptable but for the desired performance of the printer this had to be addressed.

15. **High-resolution printing**
    Goal: Improve fluidity of stepper-motors and improve resolution of printer
    Description: In order to improve the resolution of the printer, the stepper motors were upgraded. The stepper motors that were available for use in the lab were 1.8^o bi-polar stepper motors. Similar geometric test were conducted with the new stepper motors including printing circles.
    Results: The resolution of the upgraded printer was significantly improved

by upgrading the stepper motors. Based on the size of the gear on the motor and measurement verification, there are 19 steps of the stepper motor per millimeter. Thus the minimum feature size is 1/19 mm or approximately 53 μm.

16. **Causes of air pockets in layers**
    Goal: Determine the cause of buried bubbles in sintered substrates
    Description: Based on the cross section of the material shown in Figure B.4 that was dried in Experiment 12 at 150^{o}C, the cause of the air bubbles needed to be determined in order to create layers that didn't have a large amount of air. The main cause was thought to be air introduced to the slurry from mixing the slurry before use.
    Results: In order to determine the cause of the air bubbles, the slurry was placed in a vacuum environment after being mixed and placed in a syringe. Once the air bubbles were no longer escaping from the slurry, the syringe was removed from the vacuum chamber and prepared for printing. The resulting printed material was free of air bubbles. The same result can also be achieved by vacuuming the layer after it has been printing.

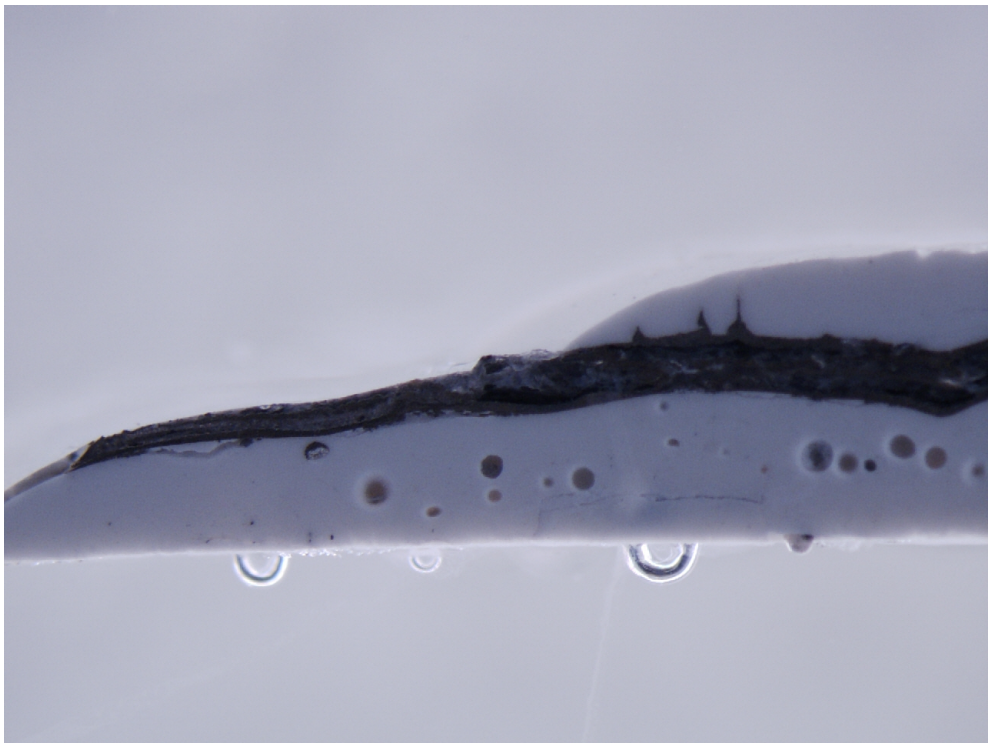

Figure B.4: Cross-section showing air pockets in un-vacuumed, sintered sample

17. **Ring resonator on Al_2O_3**
    Goal: Verify printer functionality as well as test design on material similar to LTCC
    Description: Before printing silver traces on the LTCC material, the printer's ability to dispense silver adequately was verified on alumina sheets. The goal was to determine the process to print silver on sheets that could easily be cleaned instead of having to print ceramic layers after each failed build. Instead the alumina sheet was wiped clean with isopropol alcohol and a wipe and was ready for another build.
    Results: A ring resonator was successfully built using the printer and tested on alumina sheets. In the process of building this device, several important process details where determined: The smaller the needle, the more air pressure required to dispense a uniform line, and the distance between the needle and the material must remain almost touching and constant otherwise the line will vary in width. Measurement results of this resonator can be found in Section 4.

18. **Ceramic printing**
    Goal: Characterize printing ceramic from the printer
    Description:Determine procedure for dispensing ceramic from the printer. Several details are required to be able to print ceramic layers: needle sizes, width of ceramic traces, building platform temperature when dispensing, required pressure, and motor speeds.
    Results: From this experiment, it was concluded that larger dispensing needles would be required to allow for the increased viscosity of ceramic slurry compared to the silver. The hot plate should also be off and cool in order to prevent the slurry from drying in the needle instead of on the platform. When this occurs the needle must be removed and cleaned out or replaced. The speed of the motors was determined by printing a line repeatedly changing the pressure and feed rate until it printed a uniform line with the desired height. When trying to print a layer of ceramic, the material tries to cohere and will pool up creating a thicker, smaller piece. As a result of the cohesion of the material, thin layers were not possible; however, if a layer was too thick, it would also crack. If a thin layer was created by hand and forced to spread out it would warp around the edges curling upwards. At this point, a ceramic layer was able to be printed but further investigations were needed to address the material properties that are causing the material to cohere.

19. **Ceramic & silver interaction post-dry**
    Goal: Eliminate cracking when printing multi-material, multi-layer devices
    Description: When printing multi-material coupons, cracking was observed

during the drying stage. The initial ceramic layer didn't crack nor would the layer of silver on top of the ceramic, but when another layer of ceramic was dispensed on top of the silver, it would crack. Furthermore this cracking would become worse during the sintering of the device.
Results: In order to attempt to eliminate the cracking of ceramic layers when they are placed ontop of silver layers, a cross-hatched plane was created. The goal of this was to create a ground plane that would appear to be a solid conductive sheet at microwave frequencies. The fired device was cracked and had defects due to non-uniform heating on the top layer. Further investigations are required to determine the mismatch in the interaction between the ceramic and the silver.

20. **Silver dry temperature**
Goal: Determine optimum drying temperature of conductive paste
Description: The silver must be dried prior to continuing to build on top of the layer. The appropriate temperature and drying process were investigated.
Results: If the silver layer is dried to hot such as at 125^{o}C it will peel away from the ceramic layer it was printed on. This was observed first hand when the silver and a thin layer of ceramic separated from the ceramic layer below. Although the separated layer was very thin (less than 9 mil) and multi-layer this effect is not desired. The silver layers are best dried using the hot plate at 80^{o}C.

21. **Alternative drying methods**
Goal: Prevent cracking during drying of ceramic layers
Description: The cracking of thicker layers originates at the divot created where the material completes drying. To try and remove this defect from the printed ceramic, alternative drying techniques were explored: a convection oven, the Vulcan oven, heat gun, and also gradient conduction heating with the hot plate.
Results: Convection heating did not remove the divot from the center of the sample and cracking still occurred; convection heating methods include the large convection oven and the Vulcan oven which controled the ramp rates to prevent thermal shock. The heat gun did remove the divot, but replaced it with a larger void caused by the air displacing the ceramic. Two gradient heating methods were explored. The first was done by using a piece of metal on the hot plate to concentrate the heat at the center of the coupon allowing the center to dry first and dry outward. The second method included the use of additional large pieces of metal to sink the heat on one side of the platform. This method did allow the piece to dry without cracking but the sample was suck on the building platform. This method would not be a sufficient solution

so further investigations where not conducted regarding drying.

22. **Copper as build platform**
    Goal: Print ceramic on copper such that it can be sintered on the same device it was printed on, eliminating the need to remove it from a building platform
    Description: The removal of the printed, dried coupon from the build platform often causes the device to break. This can be caused by any defect in the building platform causing the slurry to adhere to the build platform. In an attempt to skip the removal step, the ceramic slurry was printed directly onto a polished copper sheet. The goal was to print the ceramic onto the copper and fire the copper and ceramic together
    Results: Although this idea seemed promising, there were some complications. Copper will oxidize at a rapid rate at high temperatures. The copper was transformed from a shinny reflecting sheet before sintering into a black copper oxide coated sheet and the ceramic had also absorbed some of the copper and turned green.

23. **Increase ceramic loading in slurry**
    Goal: Prevent cracking of sintered multi-material, multi-layer devices by increasing the loading of ceramic in the slurry and as a result reducing the shrinkage of the ceramic layers during the sintering process
    Description: Thus far, there have been complications when printing ceramic and silver layers together. Initially, the cause was thought to be heating the unfired material too quickly and the material cracking due to the organic material burning out too fast. After decreasing the rates of heating to 2.5^{o}C per minute it was safe to say this was not the cause of the cracking. Upon further investigation and research, the was thought to be caused by mismatched thermal expansion of the material. include information from ceramic materials for electroincs pg 600 about how metalurgy shriks prior to ceramic and ceramic is in tension post sinter [22]. In other words, the ceramic changes size with temperature less than silver.
    Results: To determine if this was the case or not, the amount of ceramic present in the slurry was increased. By increasing the loading from 50$\%$ to 60$\%$ the material was able to be printed thinner also. In addition to aiding in thinner layers, increasing ceramic loading also reduced the bowing of the material during the sintering. Last but not least by increasing the loading of the slurry the cracking that occurred during sintering was eliminated.

24. **Ring resonator on X-200W**
    Goal: Apply methods and finding of previous experiments to build desired

device on printed material.

Description: Since the silver and ceramic layers could be printed without cracking, the next step was to print the ring resonator on printed ceramic.

Results: The initial build had an error in the fabrication resulting in the microstrip feed lines coming in contact with the ring resonator. As a result, the resonator would not resonate and the device was nothing more than a transmission line with a large mismatch in the middle. The second build was free of the defect causing the ring not to resonate but the CPW feed was slightly too wide and did not yield the desired results when measurent with the probe station. Measurement results of this resonator can be found in Section 4.